SHINING A LIGHT ON AUTOMATED **DIAPHRAGM FUNCTION QUANTIFICATION**

TOWARDS AN ULTRASOUND-BASED, **REPRODUCIBLE MEASURING TOOL**

S.Y. VAN LOOSBROEK

SHINING A LIGHT ON AUTOMATED DIAPHRAGM FUNCTION QUANTIFICATION. TOWARDS AN ULTRASOUND-BASED, REPRODUCIBLE MEASURING TOOL. A PILOT STUDY.

- Master Thesis -

Suus van Loosbroek

Student number : 4465318

May 2023

Thesis in partial fulfilment of the requirements for the joint degree of Master of Science in

Technical Medicine

Leiden University ; Delft University of Technology ; Erasmus University Rotterdam

Master thesis project (TM30004 ; 35 ECTS)

Dept. of Intensive Care, LUMC

June 2022 – May 2023

Supervisor(s):

Dr. D.J. van Westerloo, LUMC

Drs. J.E. López Matta, LUMC

Drs. C.V. Elzo Kraemer, LUMC

Dr. A. Schoe, LUMC

Dr. Ir. H. Pham, Philips Research

Ir. J. Haartsen, Philips Research

Drs. J.M. Visser, Philips Research

Thesis committee members:

Prof. Dr. Ir. R. Dekker, TU Delft (chair)

Dr. D.J. van Westerloo, LUMC

Dr. A. Schoe, LUMC

Dr. Ir. H. Pham, Philips Research

Preface

I am proud to present my Master's Thesis report in Technical Medicine. This project was a collaboration between the Intensive Care department at Leiden University Medical Center (LUMC) and Philips Research department in Eindhoven. I am grateful for the opportunity to conduct this thesis in an academic health center and an esteemed health technology company, which marks the successful conclusion of six years of both education and research on the interaction of medical and technological fields. In this thesis project, I aimed to shine a light on automated diaphragm function monitoring. I hope this research is a small step towards an ultrasound-based, reproducible diaphragm measuring tool.

I want to express my gratitude to several people who helped make this thesis possible. First, I would like to thank David and Jorge, my primary medical supervisors, for their dedication, inspiration, and enthusiasm throughout this project and for consistently contributing helpful input during our meetings that helped me move forward. Bram, thank you for the insightful criticism of my report writing, which has helped me become a better writer. Carlos, I want to thank you for your readiness and the promptness with which you always responded to my writing and inquiries.

Hoa, I would like to thank you for making this project happen by combining efforts and challenging me to see things from a different perspective. Thank you, Jaap, for our frequently prolonged meetings that consistently produced insightful conclusions and left me feeling motivated and eager to resume work. Jeffrey, as my predecessor, I realize that you have opened many doors for me in this research, for which I am very grateful. I am pleased that you remained involved in this project. Ronald, while our paths did not cross until late in the project, I want to thank you for chairing my committee and bringing valuable knowledge and experience to the table.

Oleh and Willem, thank you for being available for short discussions that provided helpful feedback. Also, a thank you to my fellow graduate students Janno, Rowan, Imane, Floor, Melissa, and Friso: I think we helped each other through the challenging periods not unknown to the graduation process by always offering a sympathetic ear or a therapeutic walk. Finally, I would like to thank the medical staff at the ICU in the LUMC for the educative clinical weeks under excellent supervision.

Unfortunately, the memorable train rides to Leiden and Eindhoven have come to an end. It is time to start a new journey.
Enjoy reading this Master's Thesis report!

Suus van Loosbroek
Leiden, May 2023

Abstract

Background: The diaphragm is poorly monitored in the Intensive care unit (ICU), despite its evident importance in respiration. Ultrasound (US) is frequently employed to evaluate diaphragm thickness (DT) and diaphragm thickening factor (DTF) but requires expertise and only covers a small diaphragm area. Therefore, advanced US (post-)processing techniques are being investigated for diaphragm applications, including speckle tracking methods.

Objective: The primary aim of this pilot study was to develop an algorithm enabling DT quantification. Second, both an existing Fourier-based (FBST) and intensity-based speckle tracking (IBST) algorithm were modified to determine their feasibility in diaphragm strain quantification.

Methods: *N*=42 right hemidiaphragm brightness mode (B-mode) US video clips of *N*=7 healthy volunteers and *N*=22 mechanically ventilated (MV) ICU patients were included. A DT quantification algorithm was developed in-house, including five anatomical line placements of which five motion modes (M-modes) were reconstructed. Blinded inter- and intra-rater reproducibility of manual DT assessment by two intensivists as performed in current clinical practice was tested. The FBST and IBST algorithms were modified to allow automated diaphragm segmentation, enabling global longitudinal strain (GLS) and strain rate (GLSR), and diaphragm movability (IBST score) assessment, respectively. DT and strain algorithm findings were validated against manual DT assessment by one intensivist with considerable experience in diaphragm US.

Results: Minimal (DT_{min}, mm) and maximal DT (DT_{max}, mm), and DTF (%) values were 1.9 ± 0.4, 2.3 ± 0.5, and 22.6 ± 10.9 in the MV patient group, and 2.2 ± 0.4, 3.7 ± 1.5 and 66.5 ± 45.0 in the volunteer group (all $p > 0.05$). Correlation of DT algorithm variables and manual expert grading were all significant, with a good correlation in DT_{max} (ICC 0.9, r or ρ 0.7, $p < 0.001$) and a moderate correlation in DT_{min} and DTF (ICC 0.7, r or ρ 0.7, $p < 0.001$ and $p = 0.001$, respectively). Inter- and intra-rater reproducibility of manual DT assessment was poor (ICC < 0.4 and r or ρ < 0.2). GLS (%) and GLSR (%/s) values were -32.0 ± 19.8 and -6.6 ± 3.8 in the patient group and -40.3 ± 17.3 and -10.4 ± 6.8 in the volunteer group, respectively (all $p > 0.05$). IBST scores were 26.2 ± 17.6 in the patient group and 68.1 ± 32.5 in the volunteer group ($p = 0.009$). IBST score values showed a good correlation with DTF (r or ρ 0.7, $p = 0.003$), and a moderate, negative correlation with DT_{min} (r or ρ -0.5, $p = 0.043$). No significant correlations were seen between the remaining manual expert DT assessment and algorithm-derived FBST and IBST variables.

Conclusion: DT quantification using the algorithm developed during this study correlated to conventional US expert assessment. Poor reproducibility of current diaphragm function quantification supports the need for such an automated assessment. The clinical value of diaphragm strain assessment using the modified FBST and IBST algorithms remains unclear. Further research involving a widely defined gold standard technique in diaphragm function quantification is warranted.

Contents

Nomenclature

Abbreviations

Abbreviation	Definition
ASV	Adaptive support ventilation
AUC	Area under the curve
AUC_{DT}	Area under the curve of diaphragm thickness signal over time
B-mode	Brightness mode
CI	Confidence interval
DD	Diaphragm dysfunction
DE	Diaphragm excursion
DT	Diaphragm thickness
DTF	Diaphragm thickening factor
$DT_{end\text{-}exp}$	Diaphragm thickness at end-expiration
$DT_{end\text{-}insp}$	Diaphragm thickness at end-inspiration
DT_{max}	Maximal diaphragm thickness
DT_{min}	Minimal diaphragm thickness
FBST	Fourier-based speckle tracking
GLS	Global longitudinal strain
GLSR	Global longitudinal strain rate
IBST	Intensity-based speckle tracking
ICC	Interclass correlation coefficient
ICU	Intensive care unit
L_s	Minimal length between diaphragm kernels (shortened state)
L_0	Maximal length between diaphragm kernels (reference state)
MV	Mechanical ventilation
M-mode	Motion mode
PEEP	Positive end-expiratory pressure
p-CMV	Pressure-controlled continuous mandatory ventilation
P_{di}	Transdiaphragmatic pressure
r	Pearson's correlation coefficient
ρ	Spearman's correlation coefficient
SD	Standard deviation
SPONT	Spontaneous ventilation mode
STE	Speckle tracking echocardiography
US	Ultrasound
VIDD	Ventilator-induced diaphragm dysfunction

1 Introduction

1.1. Diaphragm dysfunction on the Intensive Care

The diaphragm is the main respiratory muscle innervated by the phrenic nerve [1]. During inspiration, the diaphragm contracts, thickens, and pulls downward [2]. Throughout expiration, it extends passively upward [2]. Diaphragm dysfunction (DD) is characterized by a decreased ability to produce a negative intrathoracic pressure [3]. DD is frequently seen in mechanically ventilated patients in the Intensive Care Unit (ICU) [4]. Risk factors associated with DD are exposure to invasive mechanical ventilation (MV) – referred to as ventilator-induced diaphragm dysfunction (VIDD) [4] – patient-ventilator asynchronies [5], sepsis, malnutrition and drug use such as steroids and sedatives [6]. Especially when multiple of these circumstances are met, the diaphragm tissue is subjected to oxidative stress and inflammation, which impair its capacity to contract while causing atrophy [6]. Unilateral or bilateral diaphragm paralysis may be a component of DD, in which one or both hemidiaphragms are unable to contract adequately to enable effective inspiration [7]. This may be caused by diaphragm muscular issues or a lack of phrenic nerve innervation [7].

In VIDD specifically, the primary stage is defined by abnormal muscle contractility brought on by sarcomere disruption, protein dysfunction, and pathological calcium leakage within the muscle fibers [8]. This is rapidly followed by a decrease in muscle mass as a result of a disturbed protein balance [8]. Therefore, qualitative and quantitative diaphragm tissue damage precedes diaphragm weakness in severely ill, mechanically ventilated patients [8]. In patient-ventilator asynchronies, for example, when the neural inspiratory time surpasses the ventilator's inspiratory time, diaphragm contraction occurs during mechanical expiration and thus muscular lengthening [9, 10]. This results in eccentric loading and, as a result, diaphragm myotrauma [9, 10].

Overall, DD is associated with adverse patient outcomes [4, 11] and prognosis [12], including prolonged MV [4, 11], elevated lung ultrasound scores (LUS) [13], and reduced weaning [11, 14] and extubation success [4].

Given the detrimental impact of (VI)DD in critically ill, mechanically ventilated patients in the ICU, insight into diaphragm function in these patients is clinically relevant. However, diaphragm function is poorly monitored in the Intensive Care environment [3, 6, 15]. This is due in part to limited knowledge of health care personnel regarding the effect of DD on patient outcomes, as well as the inverse effect of critical illness on diaphragm function [6]. Additionally, diaphragm monitoring tools may be limited in availability, and the required expertise to adequately assess diaphragm function in critically ill patients may be lacking [6, 15]. The author discussed currently available monitoring techniques in a previous literature review (Appendix A).

1.2. Conventional ultrasound techniques in diaphragm monitoring

Ultrasound (US) or point-of-care ultrasound (POCUS) has become a favored tool in diaphragmatic monitoring in the ICU as it is non-invasive, fast, and available for bedside use [16–18]. Limitations include operator dependency and the significant amount of expertise required, demanding appropriate training [19].

It is common practice to evaluate diaphragm function in a brightness mode (B-mode, 2D) video clip

or based on a single specified anatomical scan line in motion mode (M-mode, 1D), at the zone of apposition (Figure 1.1) [20–25].

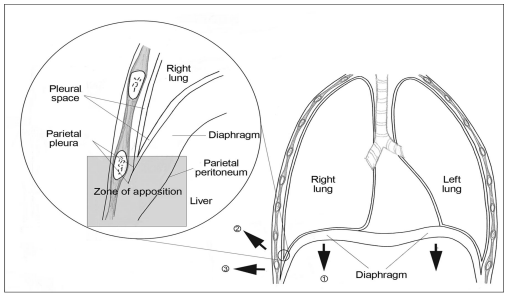

(a) Schematic view of the diaphragm in the zone of apposition by Umbrello et al. [26]

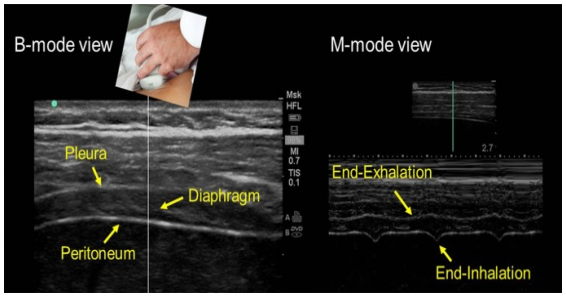

(b) Hemidiaphragm ultrasound images in brightness mode (B-mode, left) and motion mode (M-mode, right) by Laghi et al. [27]

Figure 1.1: Diaphragm ultrasound imaging in brightness mode and motion mode in zone of apposition

The hemidiaphragm is recognized as a hypoechogenic muscle layer with a hyperechogenic central tendon slip. The diaphragm tissue is located between two exaggerated hyperechogenic lines that are evident in US imaging [20, 28] and signify the pleural and peritoneal borders (Figure 1.1 and 1.2) [25].

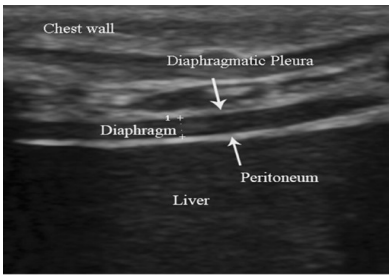

(a) Hemidiaphragm brightness mode ultrasound image in zone of apposition by Xue et al. [29]

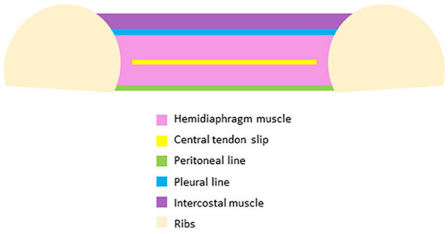

(b) Schematic view of hemidiaphragm ultrasound image in zone of apposition by Patel et al. [2]

Figure 1.2: Hemidiaphragm identification in zone of apposition during ultrasound acquisition

1.2.1. Diaphragm ultrasound parameters

US is frequently employed in the quantification of diaphragm thickness (DT, mm), diaphragm thickening factor (DTF, %), and diaphragm excursion (DE, mm) in clinical practice [30]. DT reflects diaphragm muscle size and is used to quantify diaphragm atrophy, characterized by a DT at end-expiration ($DT_{end\text{-}exp}$) smaller than 2 mm [16, 18, 20, 21, 31, 32]. DT is defined as the distance between the pleural and peritoneal borders (Figure 1.3), requiring manual measurement by the operator in the imaging device interface [25]. DTF is commonly defined as the difference between DT at end-inspiration ($DT_{end\text{-}insp}$) and $DT_{end\text{-}exp}$, according to the following formula [17, 21, 22, 32] (Figure 1.3):

$$DTF = \frac{DT_{end\text{-}inspiration} - DT_{end\text{-}expiration}}{DT_{end\text{-}expiration}} * 100 \tag{1.1}$$

DTF is associated with diaphragm contractile activity [21]. A DTF of less than 20 % is commonly used to define DD [32, 33]. In contrast to DT and DTF, DE, defined as the maximum diaphragmatic movement during respiration [16, 32, 34–37], is not directly linked to diaphragm function parameters. Also, as opposed to DTF, reductions in DE did not correlate with reductions in transdiaphragmatic pressure (P_{di}) [22].

Bedside US diaphragm examinations are typically performed in patients receiving prolonged MV and experiencing disturbed weaning. Diaphragm function assessment may then provide insight into the cause of troubled weaning [30]. Consequently, it may contribute to the challenging decision-making regarding the patient's readiness to wean and which weaning strategy to pursue [38].

Although US is the preferred method for DT assessment, it is not without drawbacks. In clinical practice,

DT is often measured at a single spot in the zone of apposition, despite varying DT across its surface [23]. Additionally, inter- and intra-rater reproducibility may be adversely affected by the small absolute values of DT in pathological conditions. To the best of knowledge, inter-and intra-rater reproducibility has only been researched when DT values were averaged across multiple diaphragm locations or respiratory cycles [20–22, 39], or in healthy volunteers only [24, 25].

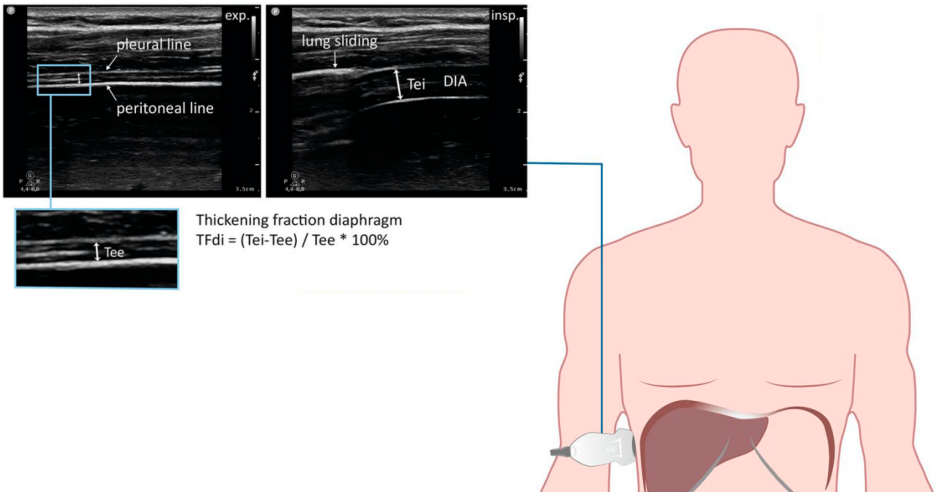

Figure 1.3: Diaphragm thickness measurements in zone of apposition by Tuinman et al. [40]. Tei, diaphragm thickness at end-inspiration; DIA, diaphragm region; Tee, diaphragm thickness at end-expiration; TFdi, diaphragm thickening factor

1.3. Diaphragm strain assessment using 2D speckle tracking echocardiography

In addition to conventional US methods, more advanced US (post-)processing techniques are being developed, one of which 2D speckle tracking echocardiography (STE). In clinical practice, this method is commonly employed in echocardiography applications [28]. Its feasibility in diaphragm function assessment is being researched [25, 28].

STE uses software to track tissue-specific grayscale pixels or speckles, produced by the interaction of muscle tissue and US beams [25]. Speckles, identified as natural acoustic markers [41], arise from the backscattering of US waves by scatterers in solid soft tissues [42, 43]. During respiration, the displacement of unique groups of speckles, termed kernels, is tracked using tracking blocks [25, 28, 44] (Figure 1.4). The movement of kernels toward one another provides insight into the behavior of myofibrils during contraction [28]. This enables strain and strain rate assessment, estimating contraction capacity [28]. Here, conventional strain (ε) and strain rate (ε') represent the relative change in length between a reference state at end-expiration (L_0) and a shortened state at end-inspiration (L), and the rate of this deformation, respectively [25, 28] (Figure 1.4):

$$\varepsilon = \frac{L - L_0}{L_0} * 100 \tag{1.2}$$

$$\varepsilon' = \frac{\Delta\varepsilon}{\Delta t} \tag{1.3}$$

A more negative number resembles a higher degree of strain, indicated by closer-spaced kernels as a result of muscle fiber shortening [25, 28].

1.4. Diaphragm strain evaluation in comparison to standard US practice

In contrast to conventional US parameters like DTF, strain and strain rate assess longitudinal diaphragm muscle shortening in the plane of muscle fiber motion [25]. However, a moderate correlation between conventional DT and strain parameters is expected based on the volume conservation principle [25].

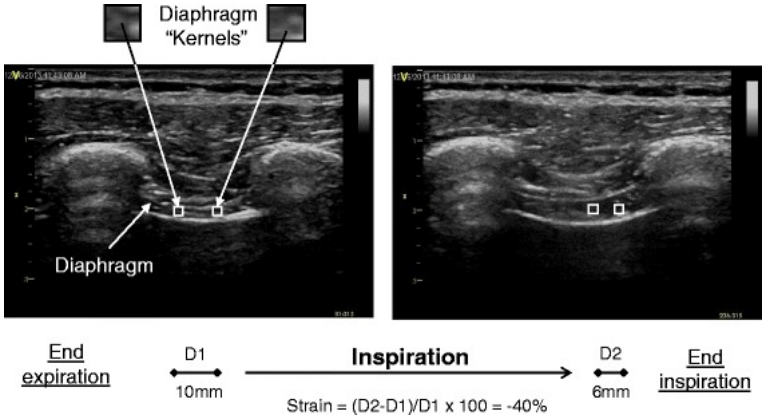

Figure 1.4: Representation of diaphragm strain assessment by Orde et al. [25]. D1 represents the reference state (L_0) and D2 the shortened state (L)

STE offers benefits over conventional US techniques. As it is a relative measurement and covers a greater area of the diaphragm on the horizontal axis, it is less reliant on the significant dispersion associated with absolute DT measurements [44]. Moreover, STE is not as operator dependent since it is less impacted by variations in probe angle during acquisition [25, 28, 44]. Despite these advantages, the use of STE in diaphragm function assessment in clinical practice is still facing challenges [28, 44]. This might be because commonly used algorithm tools, such as the 2D strain modality of EchoPac's Q-analysis tool (General Electric Healthcare) [25, 28, 45], are patented [28], complicating its availability. Moreover, STE algorithms are initially designed for myocardial applications [25, 28, 45]. This could prevent proper analysis of diaphragm function, as diaphragm morphology is not respected [28]. Consequently, tracking by the automatically generated tracking blocks may be inappropriate [25]. Additionally, some of the software's assumptions must be violated for appropriate diaphragm strain assessment. This may include a different triggering mode, using the respiratory cycle instead of the electrocardiogram signal [45]. Moreover, extended duration of analysis [45], less shallow depth application, and use of a linear array transducer instead of a phased array transducer may be required [25].

1.5. Study objectives

The first goal of this pilot study was to develop an algorithm that enables DT quantification for multiple locations at a time based on previously recorded diaphragm B-mode US video clips. The second objective was to determine the feasibility of adapting two existing speckle tracking algorithms, which were initially designed for lung sliding quantification, to allow diaphragm strain analysis. This pilot study was performed at the Leiden University Medical Center (LUMC) ICU in collaboration with Philips Research in Eindhoven.

2

Methods

2.1. Data selection

Hemidiaphragm B-mode US clips of healthy volunteers and mechanically ventilated patients admitted to the ICU of the LUMC were retrospectively obtained. Data were acquired during a prior study following the 'UTOPIA' protocol (Appendix B). All included patients were over the age of eighteen and intubated during image acquisition.
The following characteristics were obtained from the Patient Data Management System (PDMS): gender, age, primary reason for ICU admission, ventilation mode, number of days of MV at time of US acquisition, and positive end-expiratory pressure (PEEP, cmH_2O).

2.2. Diaphragm US measurement technique

In this study, the operator is characterized as the person performing the US image acquisition, while the rater is defined as the person assessing DT from the obtained US video clip.
All examinations were performed by a single operator, who was a medical student. Mechanically ventilated patients were examined supine. Healthy volunteers were examined in an upright seated position during normal, quiet breathing.
Data were obtained using the Philips Lumify (3.0) in B-mode. The L12-4 (12 to 4 MHz) transducer, a linear array probe with an aperture size of 34 mm, was used in combination with a Samsung Galaxy tablet and the Lumify app. Settings were kept as constant as possible, including a gain of 50 and a depth of 4 cm. If needed, depth was optimized to get a clear view of the diaphragm. Clip duration was set to 7 seconds. A maximal frame rate was used.
According to a standardized technique, the probe was placed in the right midaxillary line at the zone of apposition between the 8^{th} and 11^{th} intercostal space [18, 21, 31, 46]. By default, the right diaphragm side was measured as this is generally more accessible due to the acoustic window offered by the liver. Finally, dynamic images were exported and anonymized in digital imaging and communications in medicine (DICOM) format for subsequent offline imaging analysis.

2.3. DT quantification algorithm development

The in-house developed software for automated DT quantification based on diaphragm US imaging was designed by the author during this study. Algorithm development was performed in MATLAB (R2020b, MathWorks, USA). All data obtained by the algorithm were smoothed prior to performing calculations (moving average filter, smoothing factor 0.1).
A subset of the data was randomly chosen for the initial algorithm design, which was used to enhance the algorithm by repeatedly testing. After this subset's performance was satisfactory, the designed method was applied to the entire data set. The various stages of the algorithm are visualized in Figure 2.1. These actions are further explained in the following sections.

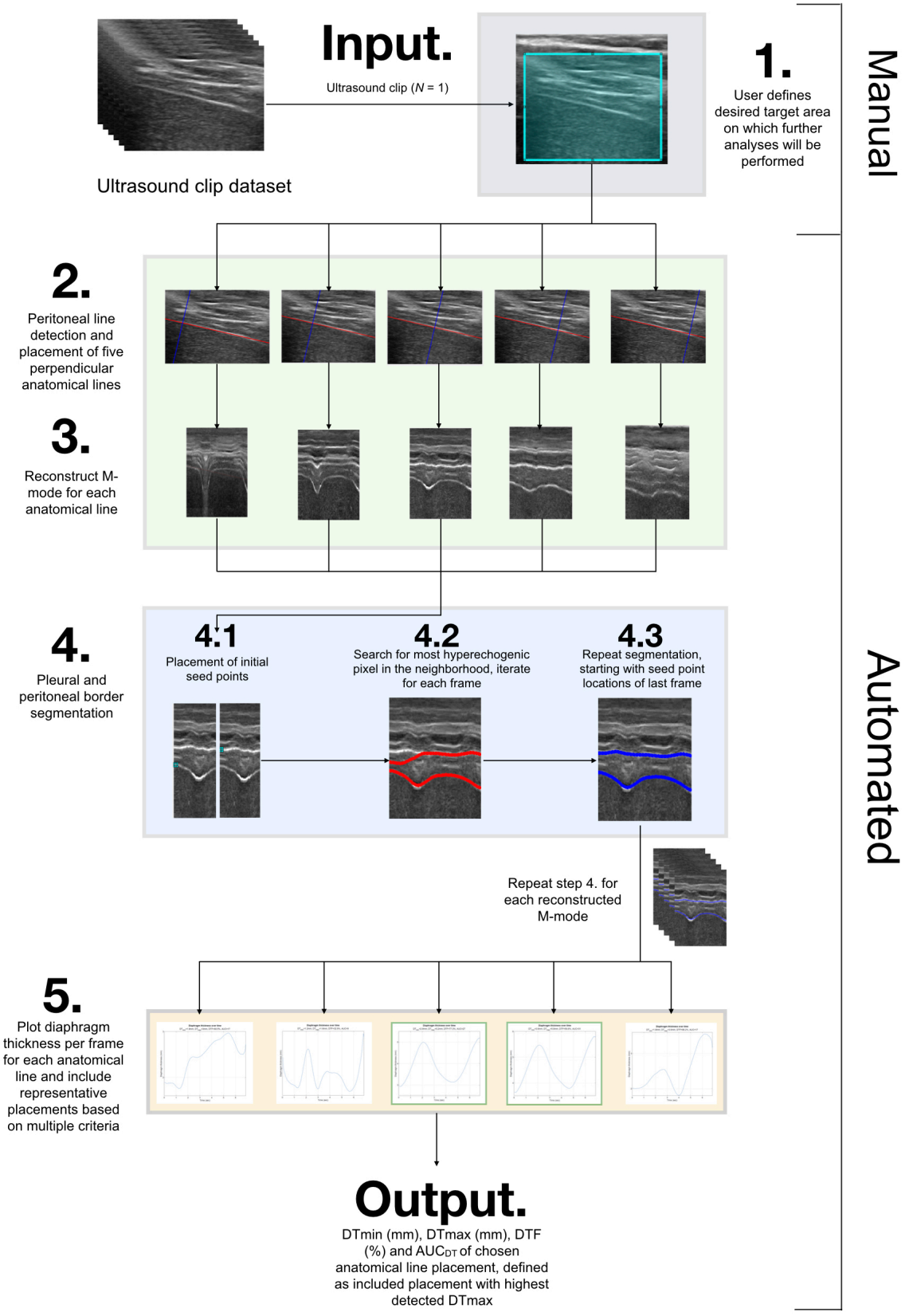

Figure 2.1: Representation of DT quantification by developed algorithm. Abbreviations: M-mode, motion mode; DT_{min}, minimal diaphragm thickness; DT_{max}, maximal diaphragm thickness; DTF, diaphragm thickening factor; AUC_{DT}, area under the curve of diaphragm thickness signal over time

Manual image cropping

An automated cropping method was initially developed but was not practicable (Table C.1, Appendix C). As a result, it was decided to continue using a manual cropping approach. The user manually defines the desired target area, which the algorithm then further analyzes. This area preferably shows a clear view of the diaphragm without interference by the rib cage or lung tissue.

Peritoneal line segmentation in first frame of B-mode clip

Peritoneal line detection in the first frame was performed using a Radon transform, which was set to detect the most distally found hyperechogenic line within the target image (visualized as a red line in Figure 2.1, Step 2). Other line detection approaches were attempted as well but did not succeed (Table C.1, Appendix C). The intensity of the detected hyperechogenic line was sampled, and outer sections with an intensity below a particular threshold were removed as they were most likely not representing the peritoneal line.

Anatomical line placements in first frame of B-mode clip and reconstruction of M-mode

Five anatomical lines were placed perpendicular to the detected peritoneal line in the first frame. These lines were evenly distributed over the total length of the peritoneal line. M-modes were reconstructed for each anatomical line, using a method developed by the author during this study.

Diaphragm thickness quantification

For each reconstructed M-mode in its first frame, the peritoneal and pleural borders were determined. Starting most distal and moving proximal, these lines were defined as the first and second hyperechogenic lines encountered, respectively. A seed point was positioned at the two identified sites.
Starting from both initial seed points placed in the first frame, the most hyperechogenic pixel in the neighborhood of the initial seed point was added to the segmentation in the next frame. This was iterated for every frame, expected to follow the pleural and peritoneal line. This method was created by the author, since widely available, open-source region growing tools were not feasible for this application (Table C.1, Appendix C).
In some cases, the central tendon was identified as the second hyperechogenic line encountered, instead of the pleural line (Figure 2.2). Therefore, a correction was applied for incorrect tendon segmentation (Figure 2.1, Step 4.2 and 4.3). As the tendon was often not constantly visible over time, it was seen that the segmentation often corrected itself and moved more proximal over time to the correct pleural line. Therefore, the segmentation was performed a second time, starting with the two initial seed points as defined in the last frame.

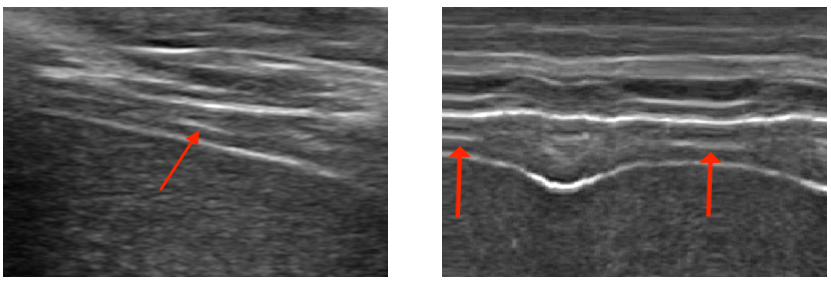

Figure 2.2: Central tendon in right hemidiaphragm ultrasound, indicated by a red arrow in B-mode (left) and its reconstructed M-mode (right)

The obtained number of pixels between the pleural and peritoneal line, representing DT per frame, was converted to millimeters. For this, the following conversion factor was used:

$$\text{Conversion factor} = \frac{\text{Depth setting (mm)}}{\text{Total number of vertical pixels of entire image (constant value)}} \tag{2.1}$$

DT variables obtained by algorithm

Due to the absence of synchronized ventilation data, no DT values could be obtained at the exact end-inspiration and end-expiration times to calculate a DTF (Section 1.2.1, Equation 1.1). Therefore,

minimal (DT_{min}) and maximal DT (DT_{max}) were computed for each clip instead of $DT_{end\text{-}exp}$ and $DT_{end\text{-}insp}$, respectively.
For each of the five reconstructed M-modes, a graph was obtained showing the DT (mm) over time with the following calculated variables as output for the entire US clip (Table 2.1): DT_{min}, DT_{max}, DTF, and the area under the curve of the DT signal over time (AUC_{DT}). The latter is a newly proposed diaphragm function parameter, thought to represent an estimate of the total amount of work performed by the diaphragm over the entire clip duration.

Selecting the anatomical line that best defines the DT variables
For each DT graph and thus anatomical line placement, several criteria were checked to determine its quality and whether the concerning anatomical line was included for further analysis. This process was performed as follows:

1. A reference graph was selected by analyzing multiple aspects of each graph. The following variables were ranked according to their weight, based on how frequently they contributed to identifying the correct graph:
    - Discard graphs with DT_{min}, DT_{max}, or DTF equal to 0 or infinitive numbers.
    - Discard graphs with pleural and peritoneal line segmentation too close to proximal and distal margins, respectively.
    - Favoring graphs when the median of the signal is close to the median of all signals combined.
    - Favoring graphs when removing the median of the signal from an array of all five medians results in the slightest difference in standard deviation (SD).
    - Favoring graphs when removing the AUC of the DT signal over time from an array of all five AUCs results in the slightest difference in SD.
    - Favoring graphs with a prominent peak in their Fourier spectrum, indicating a signal that is similar to a sinusoid.
2. After selecting the reference graph, the adjacent graphs were analyzed. These were included if they resembled the reference graph to a certain degree, considering the aforementioned criteria. Placements nearby the outer points of the diaphragm were more likely to be inaccurate compared to the center placements. Therefore, if the second placement from the left or the right did not meet the conditions and was thus excluded, the outer left or right graph was likewise discarded, respectively.

If, after completing these steps, multiple anatomical line placements were included, the placement with the highest DT_{max} was selected as the final position [18, 28]. This was thought to best represent the location where the diaphragm muscle was contracting most actively. If no anatomical line placements were included, the algorithm was unable to define an accurate DT.
Finally, the algorithm output for the selected anatomical line location consisted of the variables mentioned in Table 2.1.

Table 2.1: Variables quantified by DT algorithm

Variable	Definition
DT (mm)	Length on the vertical axis from the pleural to the peritoneal border. Divided into a minimum (DT_{min}) and a maximum value (DT_{max})
DTF (%)	Degree of thickening of diaphragm: $DTF = \frac{DT_{max} - DT_{min}}{DT_{min}} * 100$
AUC_{DT}	AUC of diaphragm thickness signal over time

Abbrevations: DT, diaphragm thickness; DT_{min}, minimal diaphragm thickness; DT_{max}, maximal diaphragm thickness; DTF; diaphragm thickening factor, AUC; area under the curve

2.4. DT quantification algorithm validation

The algorithm validation process consisted of three components: correlation to a gold standard technique as defined in this study, an agreement survey by a diaphragm US expert, and manual DT follow-

up measurement by the author. These components will be discussed in further detail in the sections below.

2.4.1. Gold standard DT technique

The gold standard technique to which the DT algorithm results were compared was defined as manual DT_{min}, DT_{max}, and subsequent DTF measurements by an intensivist experienced in US DT assessment. Visually, the timeframes where a minimal and maximal thickness was observed were selected and documented. Then, for both timeframes, a DT_{min} and DT_{max} were defined by measuring the DT at three different points on the diaphragm and averaging these values. Pleural and peritoneal line thickness were excluded from the thickness measurement. Measurements were performed using a ruler in MicroDICOM viewer (MicroDicom, Sofia, Bulgaria).

2.4.2. DT agreement survey

To define the level of agreement between DT grading by an intensivist experienced in US DT assessment and the algorithm, a survey was conducted. For the entire data set, the B-mode clips were displayed in dynamic visibility. Here, the detected peritoneal line, five anatomical lines, and the measured DT_{max} for all five sites were overlaid onto the US clip. The rater was asked to indicate whether he agreed with the algorithm evaluation based on the degree of imaging quality for each clip, meaning if the diaphragm was visualized adequately, allowing accurate DT assessment. Moreover, if applicable, the rater was requested to select the placement which resembled the most representative DT_{max} assessment. The survey was created in Powerpoint Forms. Example questions are visualized in Figures D.1 and D.2, Appendix D.

2.4.3. Manual DT follow-up measurement of the algorithm

In a subset of the data, the DT values obtained by the algorithm were compared to manually derived DT values by the author. Measurements were performed using a ruler in a DICOM viewer (Horos, Horos Project, Geneva, Switzerland). DT values were obtained at the exact same timeframes in which the algorithm calculated DT_{min} and DT_{max}. Moreover, care was taken to measure DT at a similar diaphragm location.

2.5. Inter- and intra-rater reproducibility of manual DT measurements

All B-mode clips were analyzed by two intensivists, who were blinded to each other's assessment. The raters were asked to visually determine the DT_{min} and DT_{max} at a single location of the diaphragm and to measure these variables using a ruler in MicroDICOM viewer. Pleural and peritoneal line thickness were excluded from the thickness measurement. An intra-rater reproducibility was computed by comparing the obtained variables of one intensivist with the values acquired using the gold standard technique by the same intensivist, which is outlined in Section 2.4.1.

2.6. Adaptation of speckle tracking software for diaphragm strain analysis

The in-house developed speckle tracking software designed by J.M. Visser [47] for lung sliding quantification was modified to enable diaphragm strain analysis. Algorithm adaptations were implemented in MATLAB (R2020b, MathWorks, USA). All data obtained by the algorithms were smoothed prior to performing calculations (moving average filter, smoothing factor 0.1).
Two speckle tracking techniques were used: a Fourier-based speckle tracking (FBST) and an intensity-based speckle tracking (IBST) algorithm. Solely the modifications made to these algorithms are discussed in this report. For additional details regarding their design, the author refers to the thesis report of J.M. Visser [47].

2.6.1. FBST algorithm

The FBST technique used in this study resembles the STE technique outlined in Section 1.3. Using FBST, the global longitudinal strain (GLS) of the diaphragm tissue is quantified in terms of the

differences in diaphragm length during respiration, measured by two tracking blocks. The Euclidean distance is measured between the center coordinates of the tracking blocks in each frame. The resulting frame-by-frame length measurements represent speckle displacement over time. It is expected that muscle shortening during inspiration will result in a decrease in the length between the two blocks, whilst muscle lengthening during expiration ought to result in a rise in this length.

Automated tracking block placement and size

Automated placement of two tracking blocks within the diaphragm tissue was implemented. The DT algorithm's output was employed for this. Starting from the previously identified peritoneal line, two tracking blocks were positioned at equal distances on the horizontal axis from the initially center-placed anatomical line. On the vertical axis, the blocks were moved a distance of half the DT_{min} proximally. As such, the most central portion of the diaphragm was evaluated, as more peripheral regions were often reported to produce less accurate tracking [25].
The width and height of the tracking blocks were derived empirically and set to a value of $0.5*DT_{min}$. This was expected to allow placement within the diaphragm tissue, keeping in mind the anticipated heterogeneous thickness throughout the diaphragm surface while maintaining the largest tracking block size possible to produce the most reproducible results.

Global longitudinal strain variables obtained by the algorithm

Due to the earlier mentioned absence of synchronized ventilation data, the minimal (shortened state, L_s) and maximal length (reference state, L_0) between the kernels of each clip were used, instead of the length at end-inspiration and end-expiration, respectively. Consequently, L_0 and L_s were employed to define the GLS and global longitudinal strain rate (GLSR) (Figure 2.3).

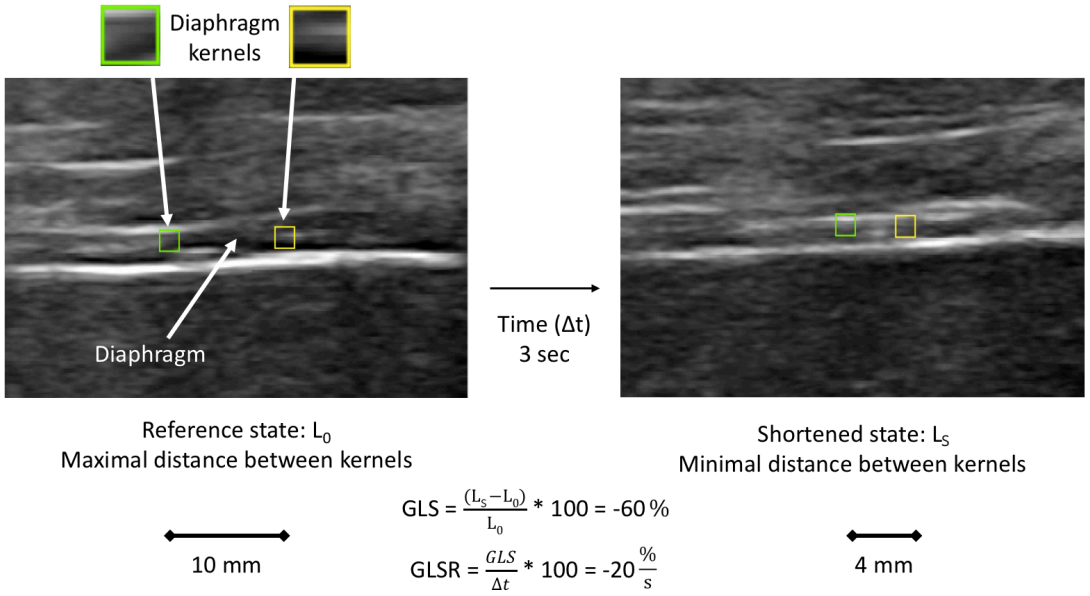

Figure 2.3: Representation of diaphragm global longitudinal strain assessment by FBST algorithm. Abbreviations: GLS, global longitudinal strain; GLSR, global longitudinal strain rate

The displacement between the two tracking blocks in relation to the reference state (L_0) was plotted over time with the following derived variables as output (Table 2.2): GLS (%) and GLSR (%/s), both defined for the entire clip.

2.6.2. IBST algorithm

In IBST, the velocity of the speckle movement is quantified in order to determine the movability of the diaphragm tissue. This degree of movability was investigated in this study in terms of its approximation of diaphragm strain. Movability analysis is enabled by assessing the magnitude of intensity changes within a predetermined tracking block. As a result, speckle movement per pixel is defined on a frame-to-frame basis.

Table 2.2: Strain variables quantified by FBST and IBST algorithm

Algorithm	Variable	Definition
FBST	GLS (%)	Relative change in length between a reference state (L_0) and a shortened state (L_s) on the horizontal axis: $GLS = \frac{L_s - L_0}{L_0} * 100$
	GLSR (%/s)	Rate of deformation: $GLSR = \frac{GLS}{\Delta t}$
IBST	IBST score	AUC of movability signal over time

Abbreviations: FBST, Fourier-based speckle tracking; GLS, global longitudinal strain; GLSR, global longitudinal strain rate; IBST, intensity-based speckle tracking; AUC, area under the curve

Automated tracking block placement and size

Using the previously defined tracking blocks in the FBST method for this application was not feasible (Table C.1, Appendix C), and therefore a new tracking block was defined. Automated placement of one tracking block within the diaphragm tissue was applied. For this, the center locations of the aforementioned FBST tracking blocks were used, where the IBST tracking block was placed in the central location between these two sites.

In contrast to the FBST approach (Section 2.6.1), pleural and peritoneal line segmentation was initially required to establish a diaphragm region on which to base further computations. This demanded a larger tracking block size to fully integrate the pleural and peritoneal borders, including additional margins. The width and height of the tracking block were determined empirically and set to a value of $1.75*DT_{max}$. This was thought to incorporate the pleural and peritoneal lines completely while avoiding extraneous intercostal muscle tissue, which may trouble the assessment.

Diaphragm segmentation

Two Vesselness filters were implemented within the tracking block in order to segment the pleural and peritoneal line throughout the clip. After completing this segmentation for the entire clip, the frame with the smallest space between the segmented pleural and peritoneal border was selected. The diaphragm mask was then defined as the area between the two segmentations in the given frame. This mask was overlaid onto the US clip to carry out the computations on this target region. The procedure for defining a diaphragm mask is depicted in Figure 2.4.

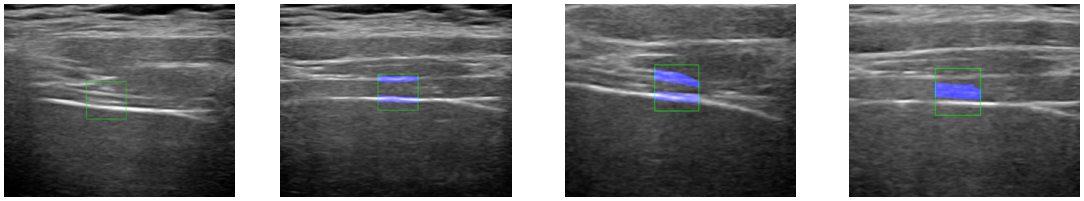

(a) Initial placement of tracking block

(b) Two Vesselness filters segmenting pleural and peritoneal borders

(c) Selected frame to define diaphragm mask

(d) Diaphragm mask

Figure 2.4: Stages of the IBST algorithm to define a diaphragm mask

Motion correction

In the original algorithm, an additional tracking block surrounding the initial tracking block was implemented for the purpose of transducer motion correction. This was enabled by tracking the adjacent muscle tissue movement and subtracting the estimated transducer motion from the measured signal of the initial tracking block. However, it was found that this method was not feasible in the diaphragm due to the thickness of the diaphragm muscle, causing exaggerated movement correction. Additionally, due to varying anatomies, it was challenging to automate the placement of this additional tracking block within the intercostal muscle area. Therefore, no motion correction was applied.

Movability variable obtained by the algorithm

The signal of all pixels within the diaphragm mask was averaged for each frame. This acquired signal was plotted over time. To define the final diaphragm movability as one value, the AUC of this signal was defined as the ISBT score (Table 2.2).
To eliminate the influence of the frame rate on the estimated movability of the diaphragm, the frame-to-frame movement was normalized using the following formula [45]:

$$\text{IBST score}_{\text{norm}} = \text{IBST score} * \frac{\text{FR}}{\text{FR}_{\text{max}}} \tag{2.2}$$

where $\text{IBST score}_{\text{norm}}$ denotes the IBST score after normalization and IBST score before normalization, FR the frame rate setting of the analyzed US diaphragm video clip, and FR_{max} the maximal frame rate setting of the entire data set.

2.7. FBST and IBST algorithm validation

Due to the lack of a manual equivalent of diaphragm strain analysis, the FBST (GLS, GLSR) and IBST (IBST score) algorithm variables were compared to the DT variables (DT_{min}, DTF) acquired by the gold standard technique as described in Section 2.4.1.

2.8. Statistical analysis

Data were analyzed using SPSS Statistics 25.0.0 (SPSS, Chicago, IL). Continuous variables were presented as mean ± SD and categorical variables as frequencies. Shapiro-Wilk test was used to test for normality. *P*-values < 0.05 were considered statistically significant. All probability values were two-sided. Continuous variables were compared using an unpaired t-test or Welch's t-test in unequal variances or Mann-Whitney U test in case of non-normal distribution. Reproducibility was expressed by the interclass correlation coefficient (ICC, two-way random effects model, mean measures, absolute agreement, 95 % CI) and Pearson's correlation coefficient (r) or Spearman's correlation coefficient (ρ) according to the distribution of the variable. Good reproducibility was defined as an ICC and r or ρ > 0.7.

3

Results

3.1. Data selection and demographics

Right hemidiaphragm B-mode US clips of *N*=7 healthy volunteers and *N*=22 mechanically ventilated patients in the ICU were included. All patients were admitted to the ICU due to respiratory failure caused by SARS-CoV-2 infection. Baseline characteristics of the mechanically ventilated patients can be found in Table 3.1. Age differed significantly between genders. No demographics of the healthy volunteers were available.

Of the mechanically ventilated patients, *N*=13 subjects were imaged two to four times, resulting in *N*=42 US clips in total. In non-pairwise comparisons, variables were averaged for double measurements. Of the *N*=35 clips of mechanically ventilated patients, ventilation modes were distributed as follows: *N*=13 (37 %) pressure-controlled continuous mandatory ventilation (P-CMV), *N*=9 (26 %) spontaneous (SPONT) ventilation, *N*=8 (23 %) INTELLiVENT adaptive support ventilation (INTELLiVENT-ASV) and *N*=5 (14 %) ASV. Frame rate settings differed across the clips between 22 and 30 frames per second (fps).

Table 3.1: Baseline characteristics of mechanically ventilated patients

Variable	All subjects (*N* = 22)	Male (*N* = 16)	Female (*N* = 6)	*P*-value
Age (years)	58.0 ± 12	54.5 ± 12	67.2 ± 7	0.025
Days on MV	10.2 ± 8	10.8 ± 8	8.8 ± 7	0.509
PEEP (cmH_2O)	11.5 ± 3	11.3 ± 3	12.2 ± 2	0.514

Abbreviations: MV, mechanical ventilation; PEEP, positive end-expiratory pressure

3.2. DT quantification algorithm variables

A subset of *N*=15 US clips was used for the initial algorithm design. Finally, the algorithm was applied to the entire data set of *N*=42 clips. Average duration of offline analysis per clip was 30 seconds.
Of *N*=11 clips, the algorithm could not compute DT variables. These clips frequently displayed ambiguous pleural and peritoneal borders, extensive adipose tissue, and acoustic shadowing. Of the remaining *N*=31 clips, DT was assessed. An example of a typical graph of diaphragm thickness over time as computed by the algorithm is depicted in Figure 3.1.

Finally, DT variables were obtained of *N*=22 clips, since *N*=9 clips were excluded. Reasons for exclusion are provided in Sections 3.3.1 and 3.3.2. DT variables for the mechanically ventilated patient group and the healthy volunteer group, as assessed by the DT quantification algorithm, are listed in Table 3.2. Additionally, all variables were compared between males and females (Table F.1, Appendix F), as well as between two measurements over time in the subjects who were imaged repeatedly (Table F.2). No significant differences were found.
The algorithm most frequently selected the three center placements out of the five locations as the most representative sites for DT calculation (Table 3.3).

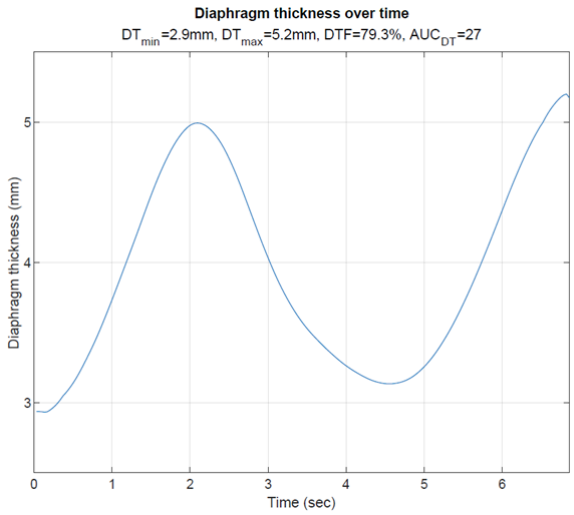

Figure 3.1: Graphical representation of right hemidiaphragm thickness (mm) over time (sec) obtained by the DT quantification algorithm. The signal shows diaphragm thickening (roughly between 0 and 2 sec, and 4.5 sec to end) and successive passive stretching. Calculated DT variables given in the subtitle: minimal (DT_{min}) and maximal diaphragm thickness (DT_{max}), diaphragm thickening factor (DTF) and area under the curve of diaphragm thickness signal over time (AUC_{DT})

Table 3.2: DT values of right hemidiaphragm by DT quantification algorithm (of in total *N*=22 clips), divided between MV patients and healthy volunteers

Variable	All subjects	Patients on MV	Volunteers	*P*-value
DT_{min} (mm)	2.0 ± 0.4	1.9 ± 0.4	2.2 ± 0.4	0.205
DT_{max} (mm)	2.7 ± 1.1	2.3 ± 0.5	3.7 ± 1.5	0.098
DTF (%)	35.5 ± 31.8	22.6 ± 10.9	66.5 ± 45.0	0.094
AUC_{DT}	16.0 ± 4.8	14.3 ± 3.0	20.2 ± 6.1	0.096

Abbreviations: MV, mechanical ventilation; DT_{min}, minimal diaphragm thickness; DT_{max}, maximal diaphragm thickness; DTF, diaphragm thickening factor; AUC_{DT}, area under the curve of diaphragm thickness signal over time

Table 3.3: Algorithm-selected placements for diaphragm thickness computation

Placement	Number of times included for analysis (%)	If included, chosen as final position (%)
1 (Most left)	27	17
2 (Second from the left)	41	78
3 (Middle)	55	50
4 (Second from the right)	59	38
5 (Most right)	27	50

3.3. DT quantification algorithm validation

3.3.1. Comparison to gold standard DT technique

N=1 clip could not be manually assessed by the rater and was therefore excluded from further analysis. Correlation between gold standard findings (defined as manual assessment by intensivist) and algorithm obtained variables DT_{max} (ICC 0.9, r or ρ 0.7, $p < 0.001$), DT_{min} and DTF (ICC 0.7, r or ρ 0.7, $p < 0.001$ and $p = 0.001$, respectively) of the total *N*=22 clips were all significant (Table 3.4, Figure 3.2).

Table 3.4: Comparison between DT variables obtained by DT quantification algorithm and by the gold standard technique (of in total *N*=22 clips)

Variable	ICC (95 % CI)	r or ρ[a]	r or ρ *p*-value
DT_{min} (mm)	0.73 (0.28 - 0.90)	0.68	<0.001
DT_{max} (mm)	0.88 (0.37 - 0.96)	0.70	<0.001
DTF (%)	0.67 (0.20 - 0.87)	0.68	0.001

[a] r or ρ used according to distribution of variable. Abbreviations: ICC, interclass correlation coefficient; 95 % CI, 95 % confidence interval; r, Pearson's correlation coefficient; ρ, Spearman's rank-order correlation coefficient; DT_{min}, minimal diaphragm thickness; DT_{max}, maximal diaphragm thickness; DTF, diaphragm thickening factor

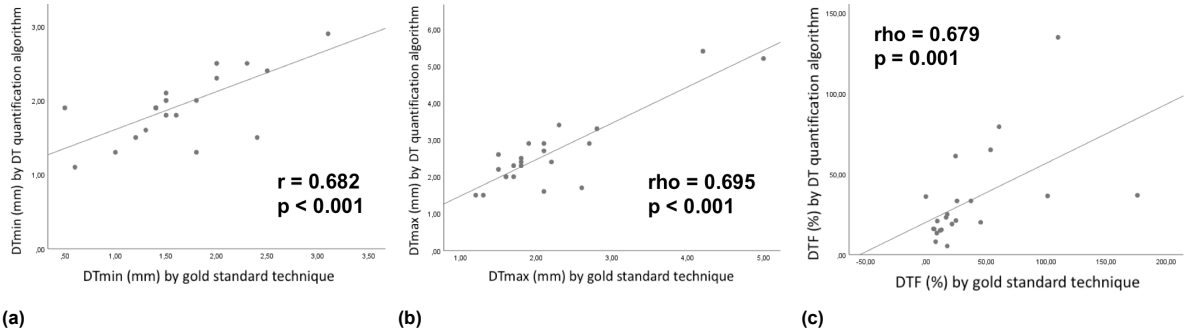

Figure 3.2: Graphical representation of correlation between DT_{min} (a), DT_{max} (b), and DTF values (c), obtained by the gold standard technique (manual expert rating) and by the DT quantification algorithm designed in this study. There was a significant correlation for all three variables. r denotes Pearson's correlaton coefficient, rho denotes Spearman's correlation coefficient

When performing the same comparison, this time only for a subset of *N*=11 clips with DT_{min} values less than 2 mm as calculated by both methods, correlation coefficient values decreased in DT_{min} and DT_{max} (Table 3.5). In contrast, DTF showed a roughly comparable, significant correlation.

Table 3.5: Comparison between DT variables obtained by DT quantification algorithm and by the gold standard technique, for a subset of *N*=11 clips with DT_{min} smaller than 2mm

Variable	ICC (95 % CI)	r or ρ	r or ρ *p*-value
DT_{min} (mm)	0.25 (-0.51 – 0.74)	0.14	0.688
DT_{max} (mm)	0.32 (-0.37 – 0.77)	0.38	0.254
DTF (%)	0.32 (-1.50 – 0.82)	0.72	0.012

For the full data set (*N*=22 clips), no correlation was observed between the time points in which the algorithm and the gold standard measured DT_{min} and DT_{max}, respectively (Table 3.6).

Table 3.6: Comparison between the time points in which the DT quantification algorithm and the gold standard technique measured DT_{min} and DT_{max} (of in total *N*=22 clips)

Variable	ICC (95 % CI)	r or ρ	r or ρ *p*-value
Time (sec) of DT_{min} measurement	-0.52 (-2.18 - 0.33)	-0.313	0.156
Time (sec) of DT_{max} measurement	-0.73 (-3.08 - 0.29)	-0.354	0.115

3.3.2. DT agreement survey

A survey was performed on all *N*=42 clips. Agreements of the algorithm and survey findings based on whether the imaging quality allowed accurate DT assessment or not are shown in Table 3.7.

Of the *N*=24 clips with sufficient quality as defined by the survey and the algorithm, the intensivist selected the exact same placement for DT assessment as chosen by the algorithm in *N*=23 out of

Table 3.7: Agreements of the algorithm and survey findings based on whether the imaging quality allowed accurate DT assessment or not (of in total *N*=42 clips)

Outcome of the algorithm	**Outcome of the survey**	
	Clip of sufficient quality	Clip quality too poor
Clip of sufficient quality	24/31 (77 %)	7/31 (23 %)
Clip quality too poor	4/11 (36 %)	7/11 (64 %)

N=24 clips (96 %). In *N*=1 case, the wrong pleural line was segmented by the algorithm, thereby overestimating the obtained DT. This clip was excluded from further analysis. Moreover, the *N*=7 clips, of which the algorithm did assess DT values but were deemed to have unacceptable imaging quality by the survey rater, were excluded from further analysis. In these cases, the diaphragm was often imaged from an incorrect angle.

US video clips that the algorithm was unable to assess, but the intensivist determined to be of sufficient quality, frequently showed lung tissue within imaging view, pushing away the diaphragm during respiration. Moreover, interference of the rib cage or a challenging imaging angle for analysis troubled algorithm assessment. Common DT algorithm errors and challenges are summarized in Figures E.1 and E.2, Appendix E.

3.3.3. Manual DT follow-up measurement of the algorithm

Manual follow-up measurements were performed on *N*=8 randomly selected US clips. The correlation for DT_{max} was significant (ICC 0.9, r or ρ 0.9, $p = 0.002$) (Table 3.8). For DT_{min} and DTF, no significant correlations were found (ICC 0.8, r or ρ 0.6, $p = 0.153$ and ICC 0.7, r or ρ 0.5, $p = 0.233$).

Table 3.8: Reproducibility of manual follow-up measurement of the DT quantification algorithm obtained variables (of in total *N*=8 clips)

Variable	**ICC (95 % CI)**	**r or ρ**	**r or ρ *p*-value**
DT_{min} (mm)	0.84 (-0.19 - 0.97)	0.56	0.153
DT_{max} (mm)	0.88 (-0.10 - 0.98)	0.90	0.002
DTF (%)	0.72 (-0.58 - 0.95)	0.48	0.233

3.4. Inter- and intra-rater reproducibility of manual DT measurements

The entire data set of *N*=42 clips was manually rated by two intensivists. *N*=5 clips were excluded because they could not be manually assessed by at least one of the raters. Inter- and intra-rater reproducibility findings of the manual DT measurements of *N*=37 clips by intensivists are listed in Table 3.9.

Table 3.9: Inter- and intra-rater reproducibility of manual DT measurements by intensivists (of in total *N*=37 clips)

Variable	**ICC (95 % CI)**	**r or ρ**	**r or ρ *p*-value**
Inter-rater			
DT_{min} (mm)	-0.06 (-1.06 - 0.46)	-0.03	0.867
DT_{max} (mm)	-0.27 (-1.53 - 0.35)	0.02	0.930
DTF (%)	-0.34 (-1.59 - 0.31)	0.10	0.538
Intra-rater			
DT_{min} (mm)	0.01 (-1.35 - 0.58)	0.01	0.978
DT_{max} (mm)	-0.33 (-2.32 - 0.44)	-0.03	0.901
DTF (%)	-0.11 (-1.69 - 0.53)	-0.03	0.909

3.5. FBST diaphragm strain variables

Average duration of offline analysis per clip was 10 seconds. *N*=6 of the *N*=22 clips analysed (27 %) were excluded, of which *N*=3 because of too small tracking blocks not performing a robust measurement, and *N*=3 due to a glitch, meaning tracking block movement not representing shortening of the diaphragm muscle. No tracking blocks were incorrectly positioned in the first frame nor moved outside the diaphragm tissue at any point during the clip.
GLS variables, as assessed by the FBST algorithm, are listed in Table 3.10. No significant differences were found.

Table 3.10: Global longitudinal strain values of right hemidiaphragm by FBST algorithm (of in total *N*=16 clips), divided between MV patients and healthy volunteers

Variable	All subjects	Patients on MV	Volunteers	*P*-value
GLS (%)	-34.6 ± 18.8	-32.0 ± 19.8	-40.3 ± 17.3	0.489
GLSR (%/s)	-7.7 ± 5.0	-6.6 ± 3.8	-10.4 ± 6.8	0.211

Abbreviations: MV, mechanical ventilation; GLS, global longitudinal strain; GLSR, global longitudinal strain rate

3.6. IBST diaphragm strain variables

Average duration of offline analysis per clip was 1 minute and 10 seconds. This processing time was highly dependent on the size of the concerning tracking block. *N*=4 of the *N*=22 clips analysed (18 %) were excluded due to pleural or peritoneal line inclusion in the diaphragm mask, causing an incorrectly enhanced movability signal. Common IBST algorithm errors and challenges are summarized in Figures E.3, E.4 and E.5, Appendix E. No tracking block was incorrectly positioned in the first frame nor moved outside the diaphragm tissue at any point during the clip.
IBST scores, as assessed by the IBST algorithm, are listed in Table 3.11. A significant difference was seen between the mechanically ventilated patient group and the healthy volunteer group (p = 0.009) (Figure 3.3).

Table 3.11: IBST score values of right hemidiaphragm by IBST algorithm (of in total *N*=18 clips), divided between MV patients and healthy volunteers

Variable	All subjects	Patients on MV	Volunteers	*P*-value
IBST score	35.1 ± 26.8	26.2 ± 17.6	68.1 ± 32.5	0.009

Abbreviations: MV, mechanical ventilation; IBST, intensity-based speckle tracking

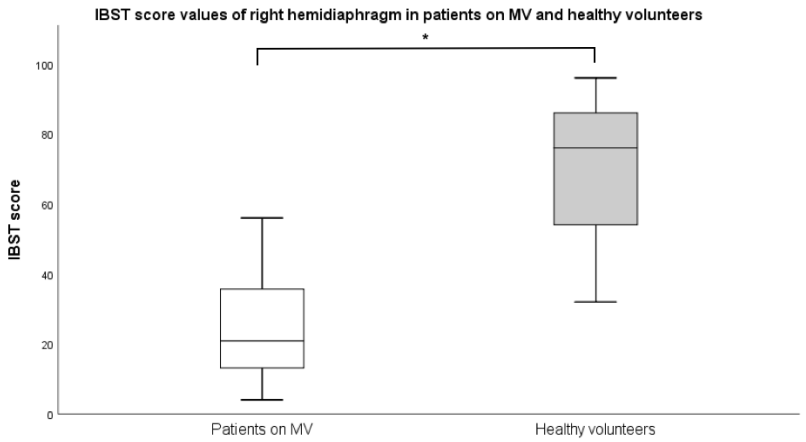

Figure 3.3: Box plot representation of IBST score values of the right hemidiaphragm (of in total *N*=18 clips) in mechanically ventilated (MV) patients and healthy volunteers. *P = 0.009 for difference between IBST score in patients on MV and healthy volunteers

3.7. FBST and IBST algorithm validation

A significant correlation was seen when comparing DTF values acquired by the gold standard technique to the IBST score values obtained by the IBST algorithm (r or ρ 0.7, p = 0.003) (Table 3.12). Moreover, a negative, significant correlation was observed when comparing DT_{min} to IBST score values (r or ρ -0.5, p = 0.043). No significant correlations were observed between the remaining DT, FBST, and IBST variables.

Table 3.12: Comparison between FBST (GLS, GLSR) and IBST (IBST score) algorithm-obtained variables and DT variables obtained by the gold standard technique

Variables	r or ρ	r or ρ *p*-value
DTF (%) and GLS (%)	-0.22	0.405
DTF (%) and IBST score	0.66	0.003
DT_{min} (mm) and GLS (%)	0.36	0.169
DT_{min} (mm) and IBST score	-0.48	0.043
GLS (%) and IBST score	-0.28	0.384
GLSR (%/s) and IBST score	-0.43	0.162

Abbreviations: r, Pearson's correlation coefficient; ρ, Spearman's correlation coefficient; DTF, diaphragm thickening factor; GLS, global longitudinal strain; IBST, intensity-based speckle tracking; DT_{min}, minimal diaphragm thickness; GLSR, global longitudinal strain rate

No correlation was observed between the time points in which the DT quantification and FBST algorithm measured DT_{min} and L_0 as well as DT_{max} and L_s, thought to represent end-expiration and end-inspiration time points, respectively (Table 3.13).

Table 3.13: Comparison of time points in which the DT quantification algorithm and FBST algorithm measured DT_{min} and L_0, respectively, as well as DT_{max} and L_s (of in total N=16 clips)

Variable	ICC (95 % CI)	r or ρ	r or ρ *p*-value
Time (sec) of DT_{min} and L_0 measurement	0.55 (-0.22 - 0.84)	0.15	0.584
Time (sec) of DT_{max} and L_s measurement	0.38 (-0.90 - 0.79)	0.24	0.366

Abbreviations: DT_{min}, minimal diaphragm thickness; L_0, reference state; DT_{max}, maximal diaphragm thickness; L_s, shortened state

3.8. Interrelation of DT, FBST and IBST variables

Examples of combined graphs of the findings of the DT, FBST, and IBST algorithms in three separate subjects are depicted in Figure 3.4. One respiratory cycle can be distinguished by a peak and valley in the signals. Here, a peak in the DT and a valley in the FBST signal suggest end-inspiration, when the diaphragm is fully thickened and shortened. Inversely, a valley in the DT and a peak in the FBST signal suggest end-expiration, when the diaphragm is more extended and flat. The IBST signal is anticipated to move in a similar manner to that of the DT and FBST signal, with no change in movability at the estimated end-inspiration and end-expiration times.

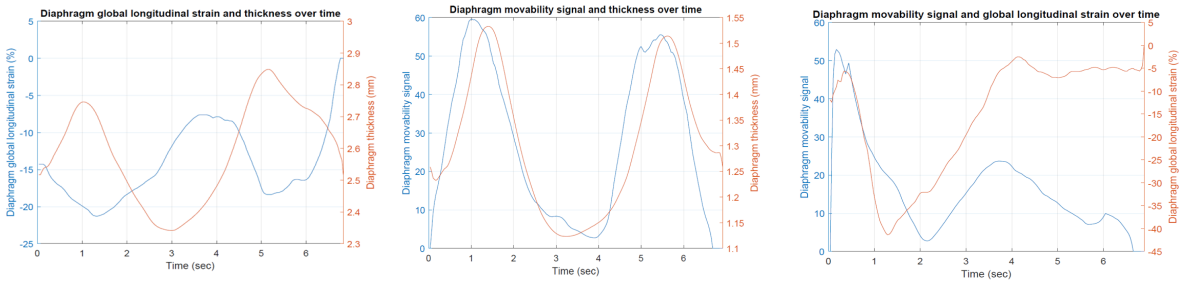

(a) DT and FBST signal **(b)** DT and IBST signal **(c)** FBST and IBST signal

Figure 3.4: Combined graphs of DT, FBST and IBST algorithm results

4

Discussion

In this pilot study, a proof-of-concept algorithm designed for US imaging was developed. This algorithm enables DT quantification for multiple diaphragm locations at a time based on a reconstructed diaphragm M-mode from a B-mode. Because of the reconstructed M-mode, correlation of both M-mode and B-mode features is enabled, and perpendicular anatomical line placement is ensured. Moreover, two existing speckle tracking algorithms, which were initially designed for lung sliding quantification, were adapted for use in diaphragm strain assessment in B-mode imaging.
Due to the manual target area selection, it is expected that minimal adjustments will be required to apply the algorithm to clips from other US imaging equipment sources. However, when doing so, the settings used, such as gain and depth, should be kept in mind and possibly compensated for. This study did not research how varied settings affected results, as these settings were largely constant across the entire data set.
When performing appropriate adaptations, the designed DT quantification algorithm may also be used in pediatric applications or in thickness quantification of other respiratory muscles, such as the lateral abdominal wall and rectus abdominis muscle [24].

4.1. DT quantification algorithm

4.1.1. Algorithm variables

Automated DT assessment using the designed algorithm was feasible. Average DT_{min}, DT_{max}, DTF, and AUC_{DT} values were 2.2 mm, 3.7 mm, 66.5 %, and 20.2 in the healthy volunteer group and 1.9 mm, 2.3 mm, 22.6 %, and 14.3 in the MV patient group, respectively.
The variables of the healthy volunteer group are similar to the values of the control group reported by Oppersma et al. (average $DT_{end\text{-}exp}$ 2.4 mm, $DT_{end\text{-}insp}$ 3.8 mm, DTF 60 %) [28]. In MV patients, average $DT_{end\text{-}exp}$ values of 2.3 to 2.4 mm are reported [23, 48], which are higher compared to the findings in this study. This may be explained by differing illness severity, ventilator settings, operator dependent factors, or the discrepancy between $DT_{end\text{-}exp}$ and DT_{min}, as well as $DT_{end\text{-}insp}$ and DT_{max}. On the contrary, Baldwin et al. reported a mean DT of 1.6 mm in MV patients, albeit solely among MV patients with sepsis [49].
In MV patients, published DTF values fluctuated substantially, from 11 to 31 % [22, 23]. The obtained DTF value of 22.6 % in this study falls within this range. As AUC_{DT} has not been reported in previously reported studies, and as it produced similar, non-significant results in mechanically ventilated patients and healthy volunteers compared to DT_{min}, DT_{max}, and DTF, its additional value remains unknown. Furthermore, due to the absence of synchronized ventilation data, AUC_{DT} was not corrected for respiratory frequency and thus may be strongly dependent on the number of breathing cycles during the US video clip.
No significant DT differences were found between the healthy volunteer group and the MV patient group, which was similarly observed by Baldwin et al. [49]. Additionally, no significant differences in DT values were seen between the two measurements over the course of MV, nor between genders. The latter is in opposition to literature findings [24, 50, 51]. However, studies frequently used a larger sample size and observed this finding in healthy volunteers only. In this study, gender differences were

only investigated in MV patients due to the missing demographic data of the healthy volunteer group. Therefore, ventilator-related factors such as MV duration and PEEP levels may have influenced the obtained DT values.

4.1.2. Algorithm validation

DT algorithm findings showed a good, significant correlation with the gold standard technique as defined in this study (DT_{max} ICC 0.9, r or ρ 0.7, $p < 0.001$; DT_{min} and DTF ICC 0.7, r or ρ 0.7, $p < 0.001$ and $p = 0.001$, respectively). Moreover, in 96 % of the assessed clips, the expert selected the exact same placement out of the five available locations as the algorithm did for DT assessment. However, based on the survey findings, the algorithm lacks the ability to determine whether the imaging quality of the proposed clip is sufficient for accurate analysis. Therefore, accurate DT assessment by the algorithm is dependent on the imaging quality of the clip, suggesting that imaging by an experienced, trained clinician in diaphragm US is required.

Based on comparison with the gold standard and manual follow-up measurements, reproducibility was highest in DT_{max}, followed by DT_{min} and DTF. DT_{min}, as the smallest absolute number, generally involved a wider dispersion, affecting reproducibility. DTF results had large standard deviations and were extremely sensitive to small changes in DT_{min} and DT_{max}. Therefore, it appears clinically relevant to consider DTF and DT_{min} jointly rather than separately. This also accounts for circumstances in which DT_{min} is normal, but only minor contraction occurs during respiration, and vice versa.

4.1.3. DT measurement locations in the zone of apposition

The question remains whether an average DT of multiple locations or selecting one site out of multiple locations with the largest detected DT_{max} is the most accurate in DT assessment. Averaging DT values of multiple locations is typically done in previously performed studies [20–22, 24]. However, in this study, a good correlation was found between manual, averaged measurements and the single chosen measurement location by the algorithm, suggesting adequate reproducibility for both methods. By all means, both approaches are not feasible in clinical practice as they are time-consuming, demanding automated assessment.

As the algorithm mainly favored the three middle locations, DT may be underestimated when incorporating outer distal measuring points. Closer to its attachment to the lower rib, the diaphragm may contract less. However, a more difficult assessment of outer locations due to interference of the lung tissue or rib cage may also be a reason for favoring center locations. In the latter case, a more advanced pleural and peritoneal border segmentation method might allow DT assessment by the algorithm with greater accuracy at outer diaphragm sites. This could then provide additional insight into appropriate DT measurement locations in the zone of apposition.

4.1.4. Reproducibility of DT measurements in diaphragm atrophy

A poor correlation between DT algorithm findings and the gold standard was observed when only including diaphragms with detected DT less than 2 mm (average ICC in all variables 0.3). This suggests that correlation of DT variables between both methods increases linearly with diaphragm function. This could be because the algorithm, manual expert grading, or both are less accurate at detecting DT in diaphragm atrophy. This should be researched using a validated gold standard technique such as transdiaphragmatic pressure (P_{di}) or diaphragm electrical activity (EA_{di}) assessment. The algorithm may need improved detection of DT in diaphragm atrophy, including a more precise correction for pleural and peritoneal border involvement.

4.1.5. Continuous diaphragm monitoring and target patient population

In this study, diaphragm parameters were measured at one single time point. However, it is unknown whether this is representative of diaphragmatic activity over a longer time [52]. Therefore, the additional value of continuous diaphragm assessment in an ICU setting should be researched. Moreover, a specific ICU patient population that may benefit from an algorithm like the one developed in this study should be identified. If continuous diaphragm monitoring of the degree of atrophy and contractility over time proves clinically significant, more reproducible measuring tools with reduced operator dependency are required.

4.2. Inter- and intra-rater reproducibility of manual DT measurements

Inter- and intra-rater reproducibility of manual DT measurements were poor (ICC < 0.4 and r or ρ < 0.2 in all cases). In contrast, published studies reported excellent inter- and intra-rater reproducibility, with an overall average ICC of 0.8 [20–22, 24, 25]. This discrepancy may be caused by several factors. First, there was no synchronized ventilation data available in this study. Therefore, end-inspiration and end-expiration times were unknown, and the intensivists had no preset time points in which to perform the measurements. Second, two methods of measurement were compared to determine intra-rater reproducibility. One method was DT measurement at a single location. This was thought to more closely resemble the clinical practice compared to the second method of averaging DT values over multiple locations. This second method is most frequently used in reported studies [20–22, 24], and may be associated with superior reproducibility findings. Third, compared to other studies, imaging quality and operator experience may have been subpar. Finally, reproducibility may be adversely affected by the measurement of smaller muscle sizes. Other studies mainly investigated healthy volunteers only, with an average $DT_{end\text{-}exp}$ of 2.4 to 3.4 mm [23, 25, 39], as opposed to the average DT_{min} of 1.9 mm in the MV group found in this study.

Overall, these results suggest that manual DT assessment of one single diaphragm location with absent end-inspiration and end-expiration times is not reproducible. As a good correlation was found between the algorithm and the gold standard findings but no correlation between the time points in which DT_{min} and DT_{max} were measured, this suggests that the location of measurement is of greater importance than the time points of measurement.

4.3. FBST and IBST diaphragm strain assessment

4.3.1. FBST and IBST variables

FBST

Average GLS and GLSR values were -32.0 % and -6.6 %/s in the mechanically ventilated patient group and -40.3 % and -10.4 %/s in the healthy volunteer group, respectively. Similarly, Orde et al. reported an average GLS of -40 % in healthy volunteers [25]. Ye et al. found an average GLS of -10 % over three diaphragm regions, although for a mixed group of *N*=6 healthy volunteers and *N*=8 mechanically ventilated patients and using a different type of speckle tracking method [45].

Oppersma et al. reported a maximum GLSR of -1.5 s^{-1} in healthy volunteers [28]. This discrepancy may be explained by the use of a different strain rate unit (s^{-1} against %/s). Moreover, Oppersma et al. used a different, instantaneous approach for strain rate calculation [28]. Because of its sensitivity to smoothing and outliers, this method was not employed in this study. Furthermore, it is important to note that in this study, GLSR may be underestimated, as it is calculated for an entire US clip rather than a single respiratory cycle. As a result, GLSR findings include a large spread, possibly affecting correlation results.

No significant differences were found between healthy volunteers and MV patients, nor between genders or between multiple measurements over time during the course of MV. As a scarce number of studies discussed diaphragm GLS assessment using an approach comparable to FBST, all using a patented algorithm tool not publicly available and studying healthy volunteers only, limited conclusions can be drawn from the GLS findings in this study.

IBST

Average IBST score findings were 26.2 in the mechanically ventilated subject group and 68.1 in the healthy volunteer group (p = 0.009). No significant differences were found between genders or during multiple measurements over time. To the best of knowledge, this technique has not yet been researched in literature for diaphragm applications.

4.3.2. FBST and IBST algorithm validation

No significant correlations were found between DT variables acquired by the gold standard technique and FBST (GLS, GLSR) variables. Similarly, Oppersma et al. found no significant correlation between GLS and DTF [28]. Orde et al. reported a weak correlation between GLS and DTF (r 0.4, p < 0.0001) [25].

It was expected that the time points of measurement of DT_{min} and L_0, and DT_{max} and L_s would roughly resemble each other, as they are thought to be approximately equivalent to end-expiration and end-inspiration times, respectively. However, no correlation was seen. This calls the validity of the FBST measurement into question.
IBST score variables showed a good, significant correlation to DTF (r or ρ 0.7, p = 0.003) and a negative, moderate, and significant correlation to DT_{min} (r or ρ -0.5, p = 0.043).
Finally, GLS, GLSR, and IBST score findings showed large standard deviations. Overall, the clinical value of the diaphragm strain measurements obtained by the FBST and IBST algorithms remains unclear.

4.3.3. Feasibility of FBST and IBST techniques in diaphragm applications

When comparing the FBST to the IBST technique, FBST is more favorable as it most resembles the Echopac software strain tool used by multiple studies in diaphragm assessment, which is shown to be suitable for diaphragm applications [25, 28, 44]. Moreover, it is less dependent on probe movement and returns a relative percentage, which can be compared to literature findings, as opposed to the absolute IBST score. However, IBST is more stable than FBST and less noise-sensitive. A decreasing tracking block size reduces the accuracy of both approaches.
In the IBST method, high-intensity structures moving fast through the target area are decisive for the resulting IBST score. Due to the characteristic hyperechogenic central tendon slip frequently observed in diaphragm US, IBST results may have been significantly impacted by the presence of this tendon during acquisition. The same principle applies to the pleural and peritoneal lines, which may cause an incorrectly elevated signal when accidentally included in the measurement. Moreover, the IBST algorithm currently has a quite extensive computation time exceeding 1 minute, complicating its clinical viability.

Feasibility of FBST and IBST techniques in diaphragm atrophy

Since strain measurements are relative and obtained in the horizontal plane, and hence less dependent on the extensive dispersion inherent in small diaphragm muscle size, they clearly offer an advantage over absolute DT measurements. However, in the adapted FBST and IBST algorithms, accurate strain assessment was still partially dependent on the degree of muscle mass. Namely, detection of small DT values resulted in small tracking blocks, providing unreliable measurements and the need for exclusion. As a result, it was not possible to evaluate strain in diaphragm atrophy, which impacted results. In conclusion, given that the diaphragm is a thin muscle and may produce speckle patterns of poor quality as a result, speckle tracking analysis may be inappropriate in diaphragm applications.

4.4. Limitations

This study consisted of several limitations. At first, the used data set had several shortcomings. The US video clips consisted of a limited frame rate, and data acquisition was performed by a relatively inexperienced medical student with possibly insufficient US training. Consequently, many clips had to be excluded from algorithm analysis, either because the algorithm could not assess the clip or manual expert grading could not be performed. Due to the remaining small sample size, there was a lack of power. In addition, demographics of the healthy volunteer group were missing, which may have prevented the application of appropriate corrections.
Second, no synchronized ventilation data was available to determine inspiration and expiration times in the US clips. Therefore, parameters were defined per US clip instead of per respiratory cycle. Additionally, DT_{min} and L_0, and DT_{max} and L_s were obtained instead of values at predetermined end-expiratory and end-inspiratory times, respectively.
Third, no diaphragm function gold standard reference technique was used, such as P_{di} or EA_{di} measurements, to correlate with the DT, FBST and IBST measurements. The gold standard technique used in this study is not without shortcomings, as manual DT measurement in diaphragm atrophy is challenging.
Fourth, as imaging acquisition of the entire data set was performed by one operator, no inter- and intra-operator reproducibility measurements were performed. Therefore, the effect of variations in patient and probe positioning, pressure exercised on the probe, and settings such as depth or gain, which may have led to variations in pleural and peritoneal line depths, was not researched.

4.5. Recommendations

The following recommendations are made to optimize the algorithm during future research, which could help clarify the role of automated diaphragm function quantification and its clinical significance.
First, a more extensive data set with greater frame rate imaging should be acquired prospectively by multiple experts in US diaphragm function assessment.
Second, more advanced pleural and peritoneal border segmentation methods should be developed, possibly including a correction for exaggerated pleural and peritoneal borders in US. This may then enable more accurate DT assessment in diaphragm atrophy.
Third, the FBST and IBST methods should be optimized to further define their potential in diaphragm strain assessment. Suggestions for improvement are implementing a motion correction method and a more sophisticated diaphragm segmentation approach. In FBST, all speckles within this segmented region may then be analyzed and averaged using multiple tracking blocks, improving reproducibility.
Fourth, a method should be defined to synchronize and simultaneously visualize the ventilation with the US data. As a result, the algorithm software may be adapted so that it is triggered by the breathing cycle, where automatic identification of the start of inspiration starts US analysis. Also, ventilation parameters such as work of breathing or esophageal pressure may be obtained per breathing cycle and compared to DT and strain measurements to define the share of the mechanical ventilator.
Finally, a widely accepted gold standard technique, such as P_{di} or EA_{di} assessment, should be employed to correlate with the DT, FBST and IBST measurements. This may shed light on the potential clinical significance of FBST and IBST algorithm-derived parameters.

References

[1] Hidetaka Hamasaki. “Effects of diaphragmatic breathing on health: a narrative review”. In: *Medicines* 7.10 (2020), p. 65.

[2] Zaid Patel et al. “Diaphragm and phrenic nerve ultrasound in COVID-19 patients and beyond: imaging technique, findings, and clinical applications”. In: *Journal of Ultrasound in Medicine* 41.2 (2022), pp. 285–299.

[3] Martin Dres and Alexandre Demoule. “Diaphragm dysfunction during weaning from mechanical ventilation: an underestimated phenomenon with clinical implications”. In: *Critical care* 22.1 (2018), pp. 1–8.

[4] Yung-Yang Liu and Li-Fu Li. “Ventilator-induced diaphragm dysfunction in critical illness”. In: *Experimental Biology and Medicine* 243.17-18 (2018), pp. 1331–1339.

[5] Bulleri Enrico et al. “Patient-ventilator asynchronies: types, outcomes and nursing detection skills”. In: *Acta Bio Medica: Atenei Parmensis* 89.Suppl 7 (2018), p. 6.

[6] Jonne Doorduin et al. “Monitoring of the respiratory muscles in the critically ill”. In: *American journal of respiratory and critical care medicine* 187.1 (2013), pp. 20–27.

[7] Shane M O’Toole and Jeremy Kramer. “Unilateral diaphragmatic paralysis”. In: (2020).

[8] Basil J Petrof. “Diaphragm weakness in the critically ill: basic mechanisms reveal therapeutic opportunities”. In: *Chest* 154.6 (2018), pp. 1395–1403.

[9] Bruno De Oliveira et al. “Patient–Ventilator Dyssynchrony in Critically Ill Patients”. In: *Journal of Clinical Medicine* 10.19 (2021), p. 4550.

[10] Taiga Itagaki et al. “Relationships between double cycling and inspiratory effort with diaphragm thickness during the early phase of mechanical ventilation: A prospective observational study”. In: *Plos one* 17.8 (2022), e0273173.

[11] Bruno-Pierre Dubé and Martin Dres. “Diaphragm dysfunction: diagnostic approaches and management strategies”. In: *Journal of clinical medicine* 5.12 (2016), p. 113.

[12] Irene Dot et al. “Diaphragm dysfunction in mechanically ventilated patients”. In: *Archivos de Bronconeumología (English Edition)* 53.3 (2017), pp. 150–156.

[13] Martin Dres et al. “Diaphragm dysfunction, lung aeration loss and weaning-induced pulmonary oedema in difficult-to-wean patients”. In: *Annals of Intensive Care* 11.1 (2021), pp. 1–11.

[14] Oscar Peñuelas et al. “Ventilator-induced diaphragm dysfunction: translational mechanisms lead to therapeutical alternatives in the critically ill”. In: *Intensive care medicine experimental* 7 (2019), pp. 1–25.

[15] Leo MA Heunks, Jonne Doorduin, and Johannes G Van Der Hoeven. “Monitoring and preventing diaphragm injury”. In: *Current opinion in critical care* 21.1 (2015), p. 34.

[16] Mohammad Ghasem Hanafi, Hasan Kiani, and Mahboobeh Rashidi. “Evaluation of diaphragm dysfunction to predict extubation time of critically ill patients in ICU with ultrasonography”. In: *Pakistan Journal of Medical and Health Sciences* 14.2 (2020), pp. 911–915.

[17] Ernest DiNino et al. “Diaphragm ultrasound as a predictor of successful extubation from mechanical ventilation”. In: *Thorax* 69.5 (2014), pp. 431–435.

[18] Bram Kilapong et al. “Diaphragm muscle thinning in mechanically ventilated critically ill patients”. In: *JPMA. The Journal of the Pakistan Medical Association* 71.2 (2021), S78–S83.

[19] Agnieszka Lewińska and Karen Shahnazaryan. “The use of diaphragm ultrasonography in pulmonary physiotherapy of COPD patients: a literature review”. In: *Journal of Clinical Medicine* 9.11 (2020), p. 3525.

[20] Colin Anthony Francis, Joaquín Andrés Hoffer, and Steven Reynolds. “Ultrasonographic evaluation of diaphragm thickness during mechanical ventilation in intensive care patients”. In: *American Journal of Critical Care* 25.1 (2016), e1–e8.

[21] Zhihua Lu et al. “Alterations in diaphragmatic function assessed by ultrasonography in mechanically ventilated patients with sepsis”. In: *Journal of Clinical Ultrasound* 47.4 (2019), pp. 206–211.

[22] Michele Umbrello et al. “Diaphragm ultrasound as indicator of respiratory effort in critically ill patients undergoing assisted mechanical ventilation: a pilot clinical study”. In: *Critical Care* 19 (2015), pp. 1–10.

[23] Ewan C Goligher et al. “Measuring diaphragm thickness with ultrasound in mechanically ventilated patients: feasibility, reproducibility and validity”. In: *Intensive care medicine* 41 (2015), pp. 642–649.

[24] Mark E Haaksma et al. “Anatomical variation in diaphragm thickness assessed with ultrasound in healthy volunteers”. In: *Ultrasound in Medicine & Biology* 48.9 (2022), pp. 1833–1839.

[25] Sam R Orde et al. “Diaphragm assessment by two dimensional speckle tracking imaging in normal subjects”. In: *BMC anesthesiology* 16.1 (2015), pp. 1–8.

[26] Michele Umbrello and Paolo Formenti. “Ultrasonographic assessment of diaphragm function in critically ill subjects”. In: *Respiratory Care* 61.4 (2016), pp. 542–555.

[27] Franco A Laghi, Marina Saad, and Hameeda Shaikh. “Ultrasound and non-ultrasound imaging techniques in the assessment of diaphragmatic dysfunction”. In: *BMC Pulmonary Medicine* 21.1 (2021), pp. 1–29.

[28] Eline Oppersma et al. “Functional assessment of the diaphragm by speckle tracking ultrasound during inspiratory loading”. In: *Journal of applied physiology* 123.5 (2017), pp. 1063–1070.

[29] Yang Xue et al. “A prospective observational study on critically ill children with diaphragmatic dysfunction: clinical outcomes and risk factors”. In: *BMC pediatrics* 20 (2020), pp. 1–7.

[30] Jung-Wan Yoo et al. “Comparison of clinical utility between diaphragm excursion and thickening change using ultrasonography to predict extubation success”. In: *The Korean journal of internal medicine* 33.2 (2018), p. 331.

[31] Tom Schepens et al. “The course of diaphragm atrophy in ventilated patients assessed with ultrasound: a longitudinal cohort study”. In: *Critical care* 19 (2015), pp. 1–8.

[32] Eman Ramzy Ali and Ahmad Mostafa Mohamad. “Diaphragm ultrasound as a new functional and morphological index of outcome, prognosis and discontinuation from mechanical ventilation in critically ill patients and evaluating the possible protective indices against VIDD”. In: *Egyptian Journal of Chest Diseases and Tuberculosis* 66.2 (2017), pp. 339–351.

[33] Ewan C Goligher et al. “Mechanical ventilation–induced diaphragm atrophy strongly impacts clinical outcomes”. In: *American journal of respiratory and critical care medicine* 197.2 (2018), pp. 204–213.

[34] Funda Gok et al. “Diaphragm and lung ultrasonography during weaning from mechanical ventilation in critically ill patients”. In: *Cureus* 13.5 (2021).

[35] Lucie Fenet Mariani et al. “Ultrasonography for screening and follow-up of diaphragmatic dysfunction in the ICU: a pilot study”. In: *Journal of Intensive Care Medicine* 31.5 (2016), pp. 338–343.

[36] Muhammad Tariq Khan et al. “Comparing ultrasound-based diaphragmatic excursion with rapid shallow breathing index as a weaning predictor”. In: *Cureus* 10.12 (2018).

[37] Aikaterini Flevari et al. “Diaphragmatic ultrasonography as an adjunct predictor tool of weaning success in patients with difficult and prolonged weaning.” In: *Minerva anestesiologica* 82.11 (2016), pp. 1149–1157.

[38] Ravi Saravanan et al. “Role of diaphragm ultrasound in weaning mechanically ventilated patients: A prospective observational study”. In: *Indian Journal of Anaesthesia* 66.8 (2022), pp. 591–598.

[39] Emmanuel Vivier et al. “Atrophy of diaphragm and pectoral muscles in critically ill patients”. In: *Anesthesiology* 131.3 (2019), pp. 569–579.

[40] Pieter R Tuinman et al. “Respiratory muscle ultrasonography: methodology, basic and advanced principles and clinical applications in ICU and ED patients—a narrative review”. In: *Intensive care medicine* 46 (2020), pp. 594–605.

[41] Xiong Ye et al. “Two-dimensional strain ultrasound speckle tracking as a novel approach for the evaluation of right hemidiaphragmatic longitudinal deformation”. In: *Experimental and therapeutic medicine* 6.2 (2013), pp. 368–372.

[42] Eno Hysi et al. “Insights into photoacoustic speckle and applications in tumor characterization”. In: *Photoacoustics* 14 (2019), pp. 37–48.

[43] Nick Bottenus et al. “Resolution and speckle reduction in cardiac imaging”. In: *IEEE transactions on ultrasonics, ferroelectrics, and frequency control* 68.4 (2020), pp. 1131–1143.

[44] N Hatam et al. “A novel application for assessing diaphragmatic function by ultrasonic deformation analysis in noninvasively ventilated healthy young adults”. In: *Ultraschall in der Medizin-European Journal of Ultrasound* 35.06 (2014), pp. 540–546.

[45] Xiong Ye et al. “A novel normalized cross-correlation speckle-tracking ultrasound algorithm for the evaluation of diaphragm deformation”. In: *Frontiers in Medicine* 8 (2021), p. 612933.

[46] David Cohn et al. “Diaphragm thickening during inspiration”. In: *Journal of Applied Physiology* 83.1 (1997), pp. 291–296.

[47] Jeffrey Visser. *From the seashore to the stratosphere: A step closer to continuous lung monitoring using wearable ultrasound*. `http://resolver.tudelft.nl/uuid:7e7e96da-91b1-4bdb-b7d6-7b1fefd5c462`. 2022.

[48] Michael C Sklar et al. “Association of low baseline diaphragm muscle mass with prolonged mechanical ventilation and mortality among critically ill adults”. In: *JAMA network open* 3.2 (2020), e1921520–e1921520.

[49] Claire E Baldwin and Andrew D Bersten. “Alterations in respiratory and limb muscle strength and size in patients with sepsis who are mechanically ventilated”. In: *Physical therapy* 94.1 (2014), pp. 68–82.

[50] Alain Boussuges et al. “Ultrasound assessment of diaphragm thickness and thickening: reference values and limits of normality when in a seated position”. In: *Frontiers in Medicine* (2021), p. 1982.

[51] François Bellemare, Alphonse Jeanneret, and Jacques Couture. “Sex differences in thoracic dimensions and configuration”. In: *American journal of respiratory and critical care medicine* 168.3 (2003), pp. 305–312.

[52] Ewan C Goligher et al. “Evolution of diaphragm thickness during mechanical ventilation. Impact of inspiratory effort”. In: *American journal of respiratory and critical care medicine* 192.9 (2015), pp. 1080–1088.

A

Literature review

Strategies for diaphragm function quantification of mechanically ventilated, critically ill patients in an Intensive Care setting: Prognostic and therapeutic implications. A narrative review.

Loosbroek, S.Y. van[a]

[a] MSc Student Technical Medicine, Delft University of Technology, Erasmus medical Center Rotterdam and Leiden University Medical Center Leiden, The Netherlands

Abstract

Diaphragm dysfunction in mechanically ventilated critically ill patients in the Intensive Care is associated with adverse effects on clinical outcome. Therefore insight into diaphragm function in these patients is of clinical relevance. However, diaphragm function is as of now poorly monitored in the Intensive Care environment. This narrative review provides an overview of potential techniques that may be used to assess diaphragm function as well as the prognostic and therapeutic implications of diaphragm monitoring on the course of mechanical ventilation. Several techniques will be discussed. Ultrasonography is one of the techniques with great potential and has become a favorable tool in diaphragmatic monitoring in the Intensive Care, as it is noninvasive, fast and accessible for bedside use. Most often, diaphragm ultrasonography markers consist of quantification of diaphragm thickness, diaphragm thickening factor and diaphragm excursion. Furthermore, speckle tracking ultrasonography is a novel method currently researched for diaphragm applications, enabling diaphragm deformation analysis. However, this technique is not yet researched in mechanically ventilated patients and currently used algorithms are designed for cardiac applications, demanding further research focused on the implementation of this technique in diaphragm ultrasonography. Finally, the routine implementation of functional diaphragm monitoring in mechanically ventilated patients may be of use to optimize treatment e.g. by guiding ventilator settings and weaning schemes at the bedside.

Introduction

The diaphragm is the main respiratory muscle and is innervated by the phrenic nerve (1). Diaphragm dysfunction (DD), defined as reduced capacity of the diaphragm to produce inspiratory pressure (2), is a frequently observed phenomenon in the Intensive Care Unit (ICU) in mechanically ventilated patients (3). Risk factors associated with DD are exposure to mechanical ventilation (MV) as such – referred to as Ventilator-Induced Diaphragm Dysfunction (VIDD) (3) - sepsis, malnutrition and drug use (e.g. steroids and sedatives) (4). Especially when multiple of these conditions are met, oxidative stress and inflammation are imposed on the diaphragm tissue, affecting its ability to contract and induce atrophy (4).

In VIDD specifically, the primary stage involves disturbed muscle contractility, caused by sarcomere disruption, protein dysfunction and pathological calcium leakage within the muscle fibers (5). This is then quickly followed by a reduction in muscle size due to a disturbed protein balance (5). Therefore, both qualitative and quantitative diaphragm tissue damage precedes diaphragm weakness in critically ill, mechanically ventilated patients (5).

Consequently, DD is associated with poor prognosis (6) and patient outcomes (3, 7), including extended duration of MV (3, 7) as well as reduced weaning (7, 8) and extubation success (3). Hence, diaphragm weakness inflicted by prolonged exposure to MV increases dependence on MV, thereby maintaining diaphragm tissue impairment. Adequate timing of weaning benefits patient outcomes. Delayed weaning on the other hand entails futile, prolonged exposure to MV and its' associated complications (9, 10). Inversely, premature weaning is associated with respiratory and cardiovascular stress (11), in addition to a higher risk of extubation failure and mortality (12).

Several criteria exist to assess patients' readiness for weaning in current clinical practice, including for example hemodynamic stability and appropriate oxygenation levels (13). Moreover, a spontaneous breathing trial (SBT) and the rapid shallow breathing index (RSBI) are used as weaning predictors (14, 15).

In case of a failed SBT or other factors indicating disturbed weaning, the patient is screened for possible underlying causes, such as chronic heart failure (13), pneumonia (13) and diaphragm dysfunction (16). Consequently, diaphragm function assessment is often only consulted during disturbed weaning, when considerable diaphragm weakness may be present and left unrecognized until that point in time (4).

Given the detrimental effects of VIDD in mechanically ventilated, critically ill patients on the ICU, insight into diaphragm function in these patients is of clinical relevance. However, diaphragm function is as of now poorly monitored in the Intensive Care environment (2, 4, 17). This may be due to problems related to the monitoring technique, as well as incomprehension and misjudgment regarding the interrelation between patient outcome in critical illness and DD, demanding evidence of the clinical significance of diaphragm monitoring in the ICU (4, 17).

In this narrative review, it was sought to 1. list and describe the currently available techniques and corresponding diaphragm parameters to perform functional diaphragm assessment in critically ill, mechanically ventilated ICU patients and 2. discuss the advantages and limitations of these methods for use in clinical practice and 3. review the clinical relevance of functional diaphragm monitoring during the course of MV.

Methods

1. Search Strategy and Study Selection

An electronic search of the following searching databases was conducted: PubMed (MEDLINE), Embase, Web of Science, Emcare and Cochrane Library. The corresponding search terms are stated in Appendix A. All results were imported into EndNote X9.

The article described or provided at least one of the following:

- At least one technique to perform diaphragm function quantification in mechanically ventilated patients in an ICU setting, including corresponding diaphragm monitoring parameter(s)
- An accessible algorithm tool for automated diaphragm function quantification

The following articles were excluded (if not providing a suitable algorithm tool): reviews, meta-analyses, case reports, surveys, meeting abstract references, post hoc analyses, study protocols, evaluation proposals and articles describing a diaphragm assessment technique not covered in any of the other studies or vascular assessment of diaphragm function (i.e. blood flow or vascular resistance measurements). Moreover, articles describing animal or pediatric populations, patients receiving non-invasive ventilation (NIV) or ventilation in prone position, patients with diaphragm dysfunction (e.g. paralysis or hernia), neuromuscular disease and previous history of polyneuropathy or myopathy (other than ICU-acquired weakness) were excluded.

For duplicate exclusion, title and abstract screening and full text screening, Covidence was used as a supporting software tool. First, one investigator (S.L.) assessed all titles and abstracts. Then, full texts of the remaining studies were evaluated by the same investigator. Following full text screening, a manual search was performed including references from included studies and studies referred to by contact experts.

Results

1. Study Selection and Characteristics

The final search was performed on 27-06-2022. This resulted in a total of n=1017 references (Fig. 1). After duplicate exclusion, n=424 studies remained and were screened for title and abstract. Following title and abstract screening, n=187 studies were screened for full text. Full text screening led to a final n=42 studies included for this review. The manual search resulted in an additional n=2 studies that were included. The techniques that were independently described in solely one article and therefore excluded from further discussion in this study were Tissue Doppler Imaging, Computed Tomography (CT) and Magnetic Resonance Imaging (MRI).

Of the total n=44 included studies, the following techniques to assess diaphragm function were performed: ultrasonography (US) (n=28), pressure recordings (n=12), electromyography (EMG) (=7) and US speckle tracking echocardiography (STE) (n=3), of which the latter consisted of n=2 studies derived from the manual search.

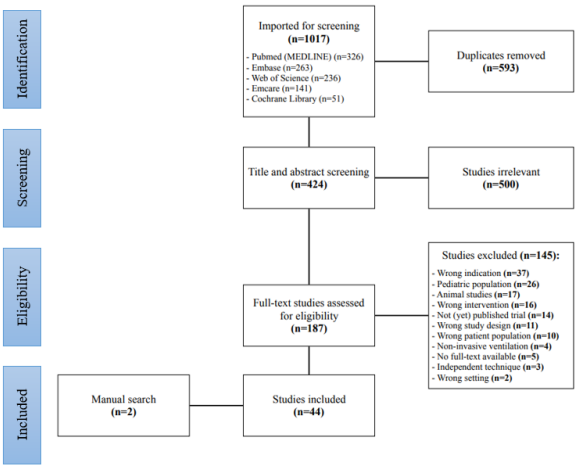

Fig 1. Flow diagram of study selection process.

2. Pressure Recordings

Assessment of transdiaphragmatic pressure (P_{di}) is considered the gold standard to assess diaphragm effort (18-20).

Using a multielectrode esophageal or nasogastric catheter equipped with pressure transducers and two air-inflated balloons, one balloon is placed in the stomach, the other in the esophagus (Fig. 2) (21, 22). Then, esophageal pressure (P_{es}) and gastric pressure (P_{ga}) are determined to define P_{di} ($P_{di} = P_{ga} - P_{es}$) (18, 21, 22).

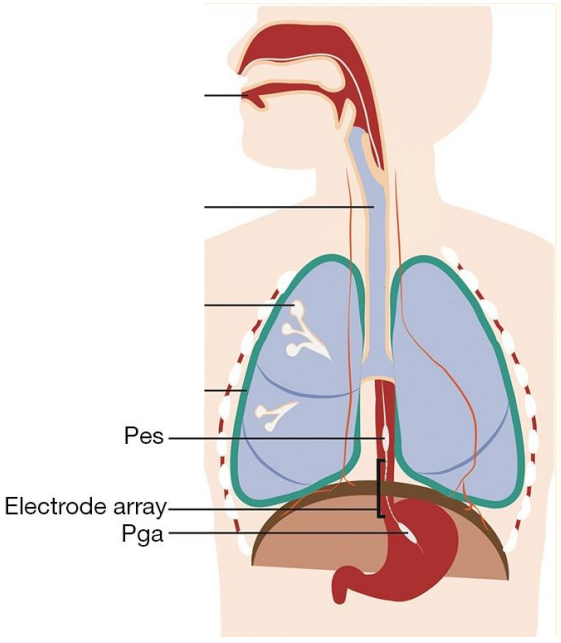

Fig. 2 Graphic visualization by de Vries et al. (23) of a pressure catheter equipped with an esophageal pressure (Pes) balloon, gastric pressure (Pga) balloon and an electrode array in between. The phrenic nerves are depicted by the orange lines.

Tidal swing in P_{di} (ΔP_{di}) or P_{di} pressure-time product (PTP) from the begin until end of inspiration may be obtained as an estimation of inspiratory effort (19, 24).

2.1 Phrenic nerve stimulation

In addition to the conventional P_{di}, transdiaphragmatic twitch pressure (twP_{di}) has been discussed to assess diaphragm strength (25). Here, twP_{di} is defined as the assessment of P_{di} in response to magnetic stimulation of the phrenic nerve during airway occlusion (18, 21, 26, 27). The latter is performed by positioning coils connected to stimulators to the sternocleidomastoid muscle (21, 28). In response to this stimulation, the diaphragm produces a negative intrathoracic pressure, of which the magnitude is proportional to the diaphragm capability to generate an inspiratory pressure (28). However, this technique is limited as the use of magnetic nerve stimulation is not feasible in all patients, due to complications of discomfort and intolerance (29).

2.2 Alternatives to transdiaphragmatic pressure assessment

Despite the evidence of P_{di} and twP_{di} being accurate markers of diaphragm effort, their clinical use is hampered by its invasiveness (20), in addition to its limited availability and complex interpretation, requiring expertise (18, 20, 26). Therefore, less invasive pressure recording techniques are proposed to assess diaphragm inspiratory effort or strength, such as tidal swing in esophageal pressure (ΔP_{es}) (19, 30) and twitch tracheal or endotracheal tube pressure (referred to as either $P_{tr,stim}$ or twP_{ett}) (27, 28, 31-33). Both techniques are more practical compared to $(tw)P_{di}$ measurements in MV patients, as they include pressure transducer incorporation on an esophageal balloon and endotracheal tube respectively, which may already be in situ in mechanically ventilated patients in the ICU (27-29). Furthermore, Buscher et al. found a strong correlation between twP_{di} and twP_{ett} (r^2=0.98) (27). However, the obtained results may be less accurate (28), as it involves a measure of inspiratory effort of the respiratory muscles combined rather than diaphragm effort specifically. Moreover, Watson et al. stated that the interrelation of twP_{di} and twP_{ett} is variable and is thereby complicating its representation of diaphragm strength in a less invasive manner (29).

3. EMG

Diaphragmatic EMG is a state of the art technique, enabling assessment of the electrical activity of the diaphragm (EA_{di}) (18). Here, EA_{di} is defined as a measure of respiratory effort (18, 34), as it indicates whether neuromuscular coupling between the brainstem and diaphragm via the phrenic nerve is intact (34). Consequently, the magnitude of the EA_{di} signal reflects real-time the patients' neural respiratory drive (34). Moreover, neurally adjusted ventilatory assist (NAVA) – a relatively new ventilation mode – employs the EA_{di} signal, in order to produce adequate ventilator settings (34).

A diaphragmatic EMG is performed by inserting a nasogastric or orogastric catheter incorporated with multiple electrodes at the level of the diaphragm (22, 34, 35). However, the use of such an EA_{di} catheter is limited by its invasiveness, poor availability and complex interpretation (18).

Pozzi et al. investigated the feasibility of non-invasive, surface EMG (sEMG) in diaphragm function assessment. Here, it was found that the EA_{di} signal was more profoundly increased in patients that failed their SBT compared to patients successfully passing their SBT ($p=0.0174$) (36). However, compared to invasive diaphragmatic EMG, a poor signal-to-noise ratio was observed (36). Similarly, using invasive EMG, Barwing et al. reported a more pronounced increase in EA_{di} signals in the patient group that failed the SBT, compared to the patients who successfully passed the SBT ($p<0.01$) (34).

4. Ultrasonography

The majority of the included studies for this review discussed conventional ultrasonography (US) techniques in diaphragm function assessment. This technique holds several advantages since it is non-invasive, portable and accessible at bedside use. All these factors together makes US a suitable tool for diaphragm monitoring in the ICU (37-39). Moreover, diaphragm US is a rapid procedure (37), generally accomplished within minutes - dependent on the patients' posture - and has a steep learning-curve (19, 39).

The diaphragm region in US imaging is visualized by tracking the exaggerated, hyperechoic lines representing the pleural and peritoneal borders (Fig. 3) (20). The central, less echogenic layer within these boundaries indicates the diaphragm (18).

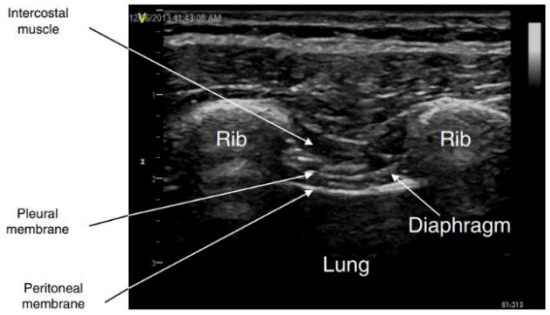

Fig. 3 Ultrasonography visualization of a normal diaphragm by Orde et al. (20), measured in the zone of apposition at the right anterior axillary line, at approximately the ninth intercostal space using a linear array transducer in M-mode.

In most studies, US measurement was performed on the right hemidiaphragm only mainly because of the acoustic window offered by the liver (37). US of the left hemidiaphragm is obscured by gastric and intestinal gas making it less accessible (24).

4.1 Diaphragm thickness

Diaphragm thickness (DT) at end expiration is frequently measured for the use of diaphragm monitoring, reflecting diaphragm muscle size (Fig. 5) (25, 37, 39-49). Consequently, DT is used to quantify diaphragm atrophy (42).

Changes in DT are common during the various stages of exposure to mechanical ventilation and may be associated with diaphragmatic weakness (40). However, Baldwin et al. found no difference in DT between septic MV patients and a healthy control group ($p=0.44$), suggesting that diaphragmatic weakness and reduction in DT may also manifest independently (49). Conversely, an increase in DT is also observed during the course of MV, although less frequent (40). When coexisting with diaphragm weakness, this may be a marker of structural injury, possibly inflicted by redundant inspiratory loads during MV, or systemic inflammation (40). However, any conclusions drawn on this finding are limited by the small patient group size (50).

Diaphragm atrophy - defined as a reduction in DT - is frequently observed in the early time course of MV (39, 42), with a maximum decrease within 72 hours following intubation (40, 43, 47). The magnitude of the reduction in DT during the time course of MV may be related to ventilation mode, as Zambon et al. reported a more pronounced daily

DT decrease in controlled MV compared to low pressure support ventilation (42).

Sklar et al. found a more pronounced and more common decrease in DT during MV in patients with a higher DT at baseline when compared to patients with a lower baseline DT (46). Therefore, monitoring of diaphragm function by the assessment of solely DT may be less accurate in patients with a low baseline DT, especially when no appropriate corrections are applied (46).

One would expect DT to be positively correlated to diaphragmatic strength. However, Supinski et al. reported a poor correlation between DT and twP_{di} ($r=0.06$, $p=0.73$) (25). No changes in DT were observed when twP_{di} indicated that diaphragm strength was remarkably decreased (25).

4.1.1 Diaphragm thickening fraction

Diaphragm thickening fraction (DTF) is a parameter derived from diaphragm thickness and defined as the relative thickening during the respiratory cycle (19, 24, 30, 35, 38, 42, 45, 47, 48, 51-53). DTF is thought to indicate diaphragm contractile activity in mechanically ventilated patients (48). DTF < 20% is reported as a definition of diaphragm dysfunction (47, 54).

In addition to the earlier described decrease in DT dependent on ventilation modes, Goligher et al. and Lassola et al. reported a positive correlation between an increase in ventilatory support and a reduction in DTF ($p<0.001$ and $p<0.0001$, respectively) (30, 53). Moreover, when decreasing the amount of ventilatory support, an increase in DTF was noted (30).

Regarding correlations with gold standard techniques, Goligher et al. described a statistically significant association between DTF and EA_{di}, with a low correlation coefficient ($r^2=0.32$, $p<0.01$) (53). Similarly, Lassola et al. reported a significant association of DTF with ΔP_{es}, also with a low correlation coefficient ($r^2=0.40$, $p<0.001$) (30). Moreover, Umbrello et al. found a significant association between DTF reductions and decreased P_{di} and P_{es} PTP with a moderate correlation coefficient ($r^2=0.49$, $p<0.001$, and $r^2=0.64$, $p<0.001$, respectively) (24).

4.2 Diaphragm excursion (DE)

Also referred to as caudal displacement, diaphragm excursion (DE) is the third, frequently employed US parameter in diaphragm functional assessment (37, 47, 51, 52, 55-59). DE is defined as the maximal distance the diaphragm moves during the respiratory cycle (Fig. 4) (37, 47, 51, 55-57). A DE < 1 cm is frequently used as a definition of diaphragm dysfunction (47, 51, 52, 55, 58, 59).

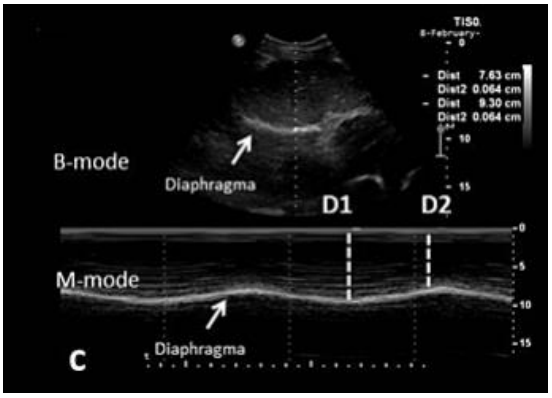

Fig. 4 Assessment of right diaphragm excursion by Gok et al. (51), in both B- and M-mode ultrasonography using a convex probe. Here, D1 = DE during inspiration and D2 = DE during expiration, where the total DE is calculated as D1-D2.

As opposed to the earlier described findings in DTF, DE did not show correlating reductions with decreased P_{di} and P_{es} PTP (24).

Table 1 displays an overview of the discussed diaphragm markers measured using US.

4.3 Weaning and extubation outcomes

Diaphragm function assessment is extensively researched in its correlation with and predictive ability of extubation (37, 38, 51, 52, 58) and weaning outcome (45, 56, 57, 59-62).

Darmawan, Er, Haji and Xu et al. all found no correlation between DE and weaning or extubation failure (45, 58, 59, 62). On the other hand, Khan, Xu and Flevari et al. all reported that a greater DE value was associated with a greater weaning success outcome or vice versa ($p<0.0001$, $p=0.014$ and $p=0.004$, respectively) (56, 57, 59). Moreover, Ghasem Hanafi et al. reported a positive correlation between reductions in both DT and DE with extubation failure ($p=0.01$ and $p=0.042$, respectively) (37). Lastly, Gok et al. found good predictive values of both DTF (PPV=95%) and DE (PPV=96%) in extubation success, nonetheless combined with sensitivity and specificity values ranging between 60 and 70 percent (51).

Table 1: Overview of parameters most often described in US diaphragm function assessment

Parameter	Probe positioning	Definition	Formula	DD definition
DT [cm]	In the right midaxillary line, at the zone of apposition, between the 8th and 11th intercostal space* (Fig. 5)	Distance from the middle of the pleural to the peritoneal border at end expiration (minimum thickness). Used to quantify diaphragm atrophy	NA	NA
DTF [%]	Similar to DT	Relative diaphragm thickening during respiratory cycle. Associated with diaphragm contractility	$\frac{DT_{end\ insp} - DT_{end\ exp}}{DT_{end\ exp}}$ x 100	DTF < 20%
DE [cm]	Lower intercostal spaces (58, 59), between midclavicular and anterior axillary lines (47, 52), US beam directed perpendicular to diaphragmatic line (55, 59) ** (Fig. 5)	Excursion amplitude, measured on vertical axis from baseline to maximum inspiration in M-mode	NA	DE < 1 cm

*DD = Diaphragm Dysfunction, DT = Diaphragm Thickness, NA = Not Applicable, DTF = Diaphragm Thickening Fraction, DE = diaphragm excursion, US = Ultrasonography. * As defined by a standardized technique first described by Cohn et al. (1997), and since then often used by others (39, 43, 48) ** No standardized technique.*

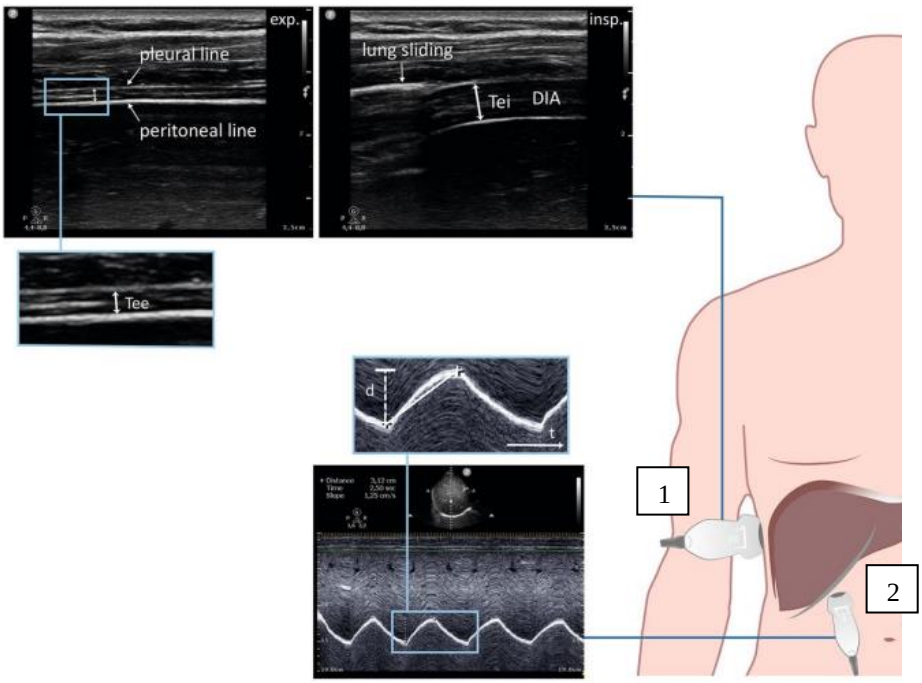

Fig. 5 Visualization by Tuinman et al. (63) of probe positioning for 1. diaphragm thickness and diaphragm thickening fraction and 2. diaphragm excursion measurement. Tee = diaphragm thickness at end expiration; Tei = diaphragm thickness at end inspiration; DIA = diaphragm area.

In some cases, diaphragm US parameters were compared to the rapid shallow breathing index (RSBI). Khan et al. stated RSBI being superior to DE in predicting weaning outcome (AUC=0.815 and 0.795, respectively; p<0.0001) (56). Moreover, Gok et al. reported a better performance of RSBI compared to DTF and DE in predicting extubation success (AUC=0.908, 0.808 and 0.792, respectively) (51). However, Flevari et al. found superior scoring in DE (AUC=0.87, p=0.001) compared to RSBI (AUC=0.77, p=0.006) when predicting weaning success (57). This discrepancy may be explained by the differences in sample size, where the sample size of the study by Flevari et al. was the smallest (n=27), compared to the studies by Khan et al. (n=90) and Gok et al. (n=62).

4.4 Reproducibility

Regarding DT, intra-observer reproducibility was reported as excellent (ICC > 0.9) (42, 43, 48, 49) and good (ICC > 0.75) (24). Similarly, inter-observer reproducibility was either stated as excellent (ICC > 0.9) (41-44, 48) or good (ICC > 0.75) (24).

Intra- and inter-observer reproducibility of DTF was defined as excellent (IC > 0.9) (38, 48). However, a moderate reproducibility was reported in DTF as well (intra- and inter-observer reproducibility 17% and 16%, respectively) (53).

In DE, a good intra-observer and inter-observer reproducibility (both ICC > 0.75) was mentioned (24).

Finally, in repetitive measurements in patients, it is advised to mark the location of the probe (53), as US measurement is limited by its dependency on the angle of the probe during acquisition (18, 20).

4.5 Non-diaphragm associated factors

The following factors are reported to be associated with reduced DT: age, sex (37), Simplified Acute Physiology Score (SAPS) II score, duration of MV, percentage of time in controlled MV modes (42), use of corticosteroids during ICU stay and sepsis (43). Hence, it may be appropriate to correct for these factors when assessing diaphragm thickness in mechanically ventilated patients.

ICU-acquired DD is described as VIDD including an additional component of diaphragm impairment related to ICU-acquired weakness (55). Therefore, associated risk-factors of ICU-acquired weakness may also be taken into account, such as neuromuscular blocking agents and aminoglycosides antibiotic use (43).

5. Speckle tracking Echocardiography

In addition to conventional US techniques, more advanced, novel US methods are being developed, of which 2D Speckle Tracking Echocardiography (STE). This technique is commonly employed in clinical practice for echocardiography applications (18). However, its feasibility in diaphragm function assessment is currently researched (18, 20).

STE makes use of software tracking tissue-characteristic grayscale pixels– referred to as “speckles” - present in muscle tissue in US images (20). The displacement of these speckles - or more specifically, unique groups of speckles called “kernels” – during a respiratory cycle is tracked, using specified regions of interest (ROI) (18, 20, 64). These ROIs are placed within the diaphragm tissue region, indicated by the two hyperechoic lines visible in US imaging (18), as described earlier.

The movement of kernels in relation to one another provides insight into the behavior of myofibrils during contraction, enabling deformation analysis (18). Consequently, quantification of the deformation parameters strain and strain rate can be quantified, providing contraction capacity estimations (18).

Strain is defined as the relative change in length between a reference (L_0) and compressed (L) state: $\varepsilon = (L - L_0)/L_0$ (18). Here, L is defined as the distance between kernels during maximal diaphragm contraction (end inspiratory state) and L_0 the distance between kernels during diaphragm relaxation (end expiratory state) (Fig. 6) (20). Accordingly, strain rate is defined as the rate of deformation: $\varepsilon' = d\varepsilon/dt$ (18).

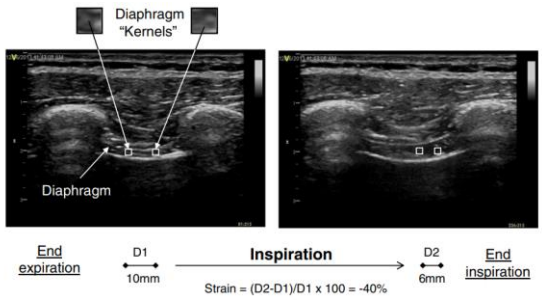

Fig. 6 Visualization of strain analysis by Orde et al. (20), representing kernel displacement during the respiratory cycle. Here, D1 = Distance between kernels at end expiration and D2 = Distance between kernels at end inspiration.

As strain is a measure of relative deformation, it comprises a negative value (20). The more negative, the higher degree of deformation, indicated by kernels coming closer together due to muscle fiber shortening (18, 20).

When comparing speckle tracking deformation parameters with conventional US markers in diaphragm monitoring, diaphragm function assessment is performed in different planes and direction (20). Here, strain and strain rate assess 'longitudinal' muscle shortening – in plane of muscle fiber motion – unlike conventional US parameters such as diaphragm thickening fraction (20). However, a moderate correlation between the two is in line with expectations based on the principle of conservation of volume (20).

Orde et al. investigated the feasibility of 2D STE US in a pilot study by the assessment of diaphragmatic strain in fifty adult, healthy volunteers (20). In addition, diaphragm excursion and diaphragm thickening fraction were measured as comparison using conventional US measurements. A weak correlation was reported between right diaphragm longitudinal strain and DTF (r^2=0.44, p<0.0001). Furthermore, poor correlations were observed between strain and DE (r^2=0.14, p<0.01) and DE and DTF (r^2=0.1, p=0.04). In DTF, DE and strain, intra- and inter-rater variability was overall acceptable (intra-rater r^2=0.9, 0.7 and 0.9, respectively (p<0.01) and inter-rater r^2=0.8, 0.9 and 0.7, respectively (p<0.01)).

Oppersma et al. performed a single point study researching the validity of 2D STE US in quantification of right diaphragm strain and strain rate during inspiratory threshold loading on thirteen adult, healthy volunteers (18). These findings were compared to P_{di}, EA_{di} and DTF measurements. They found a significant, strong correlation of P_{di} to both strain (r^2=0.72, p<0.0001) and strain rate (r^2=0.80, p<0.0001). Similarly, a significant, moderate correlation was reported between EA_{di} and both strain (r^2=0.60, p<0.0001) and strain rate (r^2=0.66, p<0.0001). Conversely, DTF did not show significant correlations with EA_{di} (p=0.790), P_{di} (p=0.495), strain (p=0.654) and strain rate (p=0.364).

STE provides several advantages in addition to conventional US: recognition of the same region of the diaphragm (18), relative independency of the probe angle during acquisition, thereby enabling more repetitive examination (18, 20, 64) and capture of a larger diaphragm area (64). Lastly, it enables differentiation of active deformation from passive movement, as kernels only move closer together during active deformation (20, 64). This may be employed in future applications to prevent patient-ventilator asynchronies (20, 64). The complex interrelation of asynchronies and diaphragm function is outside the scope of this review.

Limitations include the availability of the technique, as the concerning software algorithms are often patented (18), in addition to the substantial time the required offline data analysis takes (18, 64). As a consequence, both factors inhibit the use of diaphragm STE in clinical practice (18, 64).

Finally, Table 2 provides an overview of the discussed techniques in terms of their advantages and limitations in application of diaphragm function assessment.

Discussion

In this review, various techniques for functional diaphragm assessment in mechanically ventilated patients were discussed, as well as the clinical potential of functional diaphragm monitoring during the course of MV.

Gold standard techniques of diaphragm functional assessment include P_{di} assessment or measurement of EA_{di} by performing diaphragmatic EMG. However, these techniques are invasive, not widely available and their interpretation may be complex, requiring expertise. Therefore, less invasive variations of these methods are proposed as representation of diaphragm function, such as P_{es} measurement and sEMG. Nevertheless, such techniques may be less precise or are lacking medical evidence in depicting diaphragm function.

US has become a favorable tool in diaphragmatic monitoring in the ICU as it is noninvasive, fast and accessible for bedside use. Diaphragm US assessment commonly includes diaphragm thickness, diaphragm thickening factor and diaphragm excursion evaluation, measurements that are shown to be feasible and reproducible. It is indicated that DT or DE alone do not cover all aspects of diaphragm dysfunction, and therefore should be employed in combination with other parameters to prove clinically valuable.

Table 2: Overview of techniques for diaphragm function assessment

Method	Advantages	Limitations
Pressure Recordings	• State of the art technique	• Invasive • Not widely available • Complex interpretation
EMG	• State of the art technique	• Invasive • Not widely available • Complex interpretation
US	• Rapid • Non-invasive • Portable • Steep learning-curve • Accessible method at bedside	• Operator-dependent • Samples only small diaphragm area • Heterogeneous cut-off points • Left hemidiaphragm monitoring often not feasible
STE US	• Recognizes the same diaphragm region • Relatively operator-independent • Captures large diaphragm area • Active and passive movement differentiation	• Algorithm tools often patented • Offline data-analysis required as yet • Time-consuming

US = Ultrasonography, EMG = Electromyography, STE = Speckle Tracking Echocardiography.

A scarce number of the included studies in this review discussed speckle tracking echocardiography US, all using a patented algorithm tool not publicly available (2D strain modality of EchoPac's Q-analysis tool, General Electric Healthcare) (18, 20, 64). Therefore, limited conclusions can be drawn on its performance in diaphragm function assessment. However, STE US includes multiple advantages over conventional US – e.g. monitoring of a larger, more constant diaphragm region – making it an interesting technique to further investigate. Moreover, STE US may also be appropriate in automated quantification of conventional US markers DT, DTF and DE, albeit no studies were found to support this. Hatam et al. did research the feasibility of measuring DE using STE, but did not compare these findings with DE values obtained by a conventional US, M-mode technique (64). Therefore, further research is required to determine whether STE is useful in automated quantification of conventional US parameters. Finally, to the best of knowledge, diaphragmatic strain using STE US is not yet assessed in mechanically ventilated patients.

US diaphragm monitoring has extensively been researched in the prediction of weaning or extubation outcome, however findings are inconsistent. This may be explained by the fact that definitions of weaning failure differed throughout these studies – varying from the need for reintubation or NIV within 48 hours (38, 60) and 7 days (45) after extubation. Second, frequently only one US diaphragm parameter was researched, as opposed to its complementary role when used in addition to currently used weaning predictors or the combination with multiple US parameters. Therefore, the additional value of assessment of US diaphragm markers over SBT and RSBI findings in current practice remains unclear.

Overall, diaphragm function assessment is rarely researched in relation to long-term factors as survival outcomes, suggesting that after liberation from MV, diaphragm function is less predictive of long-term patient outcomes compared to other risk factors as for example ICU-acquired weakness (31). However, further research should be undertaken to support this hypothesis.

Routine implementation of functional diaphragm monitoring in mechanically ventilated, critically ill patients in the ICU may be used as therapeutic guidance support in the future, by guiding ventilator settings and weaning schemes at the bedside. This will enable more personalized ventilation and weaning, involving sufficient but not excessive respiratory loading, preventing muscular exhaustion. In this function, diaphragm function quantification will act as a complementary rather than an all-encompassing tool to the currently used methods, aiding clinicians in achieving adequate ventilator support and decreasing risk of weaning and extubation failure in critically ill patients.

This review was limited by the impaired comparability of the studies due to differences in diaphragm parameter definitions and heterogeneous cut-off points, complicating interpretation. Also, reproducibility measurements of the concerning parameters were not routinely performed. Moreover, limited studies compared US measurements to gold standard techniques.

Future research should focus on comparing US diaphragm function assessment methods with gold standard techniques (P_{di}, EA_{di}) as a reference. In addition, widely accepted parameter definitions and corresponding cut-off points should be defined to increase overall comparability. Furthermore, continuous US measurement may be a point of interest, possibly enabling a closed loop technique to continuously adapt ventilator settings based on diaphragm function assessment. STE US diaphragm monitoring should be researched in mechanically ventilated patients, preferably compared to a state of the art technique. Additionally, current algorithms are often patented and designed for cardiac applications, demanding widely available tools, adapted for appropriate use in diaphragm function assessment.

Conclusion

Routine implementation of functional diaphragm monitoring in mechanically ventilated, critically ill patients in the ICU may be used as therapeutic guidance support, by guiding ventilator settings and weaning schemes at the bedside. US has become a favorable tool in diaphragmatic monitoring in the ICU as it is noninvasive, fast and accessible for bedside use. Most often, diaphragm US markers consist of quantification of diaphragm thickness, diaphragm thickening factor and diaphragm excursion. Furthermore, Speckle tracking US is a novel method currently researched for diaphragm applications, enabling diaphragm deformation analysis. However, this technique is not yet researched in mechanically ventilated patients and currently used algorithms are designed for cardiac applications, demanding further research.

Abbreviations

In order of appearance: DD = Diaphragm Dysfunction; ICU = Intensive Care Unit; MV = Mechanical Ventilation; VIDD = Ventilator-Induced Diaphragm Dysfunction; SBT = Spontaneous Breathing Trial; RSBI = Rapid Shallow Breathing Index; NIV = Non-Invasive Ventilation; CT = Computed Tomography; MRI = Magnetic Resonance Imaging; US = Ultrasonography; EMG = Electromyography; STE = Speckle Tracking Echocardiography; P_{di} = Transdiaphragmatic pressure; P_{es} = Esophageal pressure; P_{ga} = Gastric pressure; PTP = Pressure-Time Product; twP_{di} = Twitch transdiaphragmatic pressure; P_{tr_stim} = Twitch tracheal pressure; twP_{ett} = Twitch endotracheal tube pressure; EA_{di} = Electrical activity of the diaphragm; NAVA = Neurally Adjusted Ventilatory Assist; sEMG = Surface EMG; DT = Diaphragm Thickness; DTF = Diaphragm Thickening Fraction; DE = Diaphragm Excursion; PPV = Positive Predictive Value; AUC = Area Under the Curve; ICC = Intraclass Correlation Coefficient; SAPS = Simplified Acute Physiology Score; ROI = Region Of Interest.

References

1. Hamasaki H. Effects of diaphragmatic breathing on health: a narrative review. Medicines. 2020;7(10):65.
2. Dres M, Demoule A. Diaphragm dysfunction during weaning from mechanical ventilation: an underestimated phenomenon with clinical implications. Critical care. 2018;22(1):1-8.
3. Liu Y-Y, Li L-F. Ventilator-induced diaphragm dysfunction in critical illness. Experimental Biology and Medicine. 2018;243(17-18):1331-9.
4. Doorduin J, van Hees HW, van der Hoeven JG, Heunks LM. Monitoring of the respiratory muscles in the critically ill. Am J Respir Crit Care Med. 2013;187(1):20-7.

5. Petrof BJ. Diaphragm Weakness in the Critically Ill: Basic Mechanisms Reveal Therapeutic Opportunities. Chest. 2018;154(6):1395-403.
6. Dot I, Pérez-Teran P, Samper M-A, Masclans J-R. Diaphragm dysfunction in mechanically ventilated patients. Archivos de Bronconeumología (English Edition). 2017;53(3):150-6.
7. Dubé B-P, Dres M. Diaphragm dysfunction: diagnostic approaches and management strategies. Journal of clinical medicine. 2016;5(12):113.
8. Peñuelas O, Keough E, López-Rodríguez L, Carriedo D, Gonçalves G, Barreiro E, et al. Ventilator-induced diaphragm dysfunction: translational mechanisms lead to therapeutical alternatives in the critically ill. Intensive Care Med Exp. 2019;7(Suppl 1):48.
9. Jung B, Vaschetto R, Jaber S. Ten tips to optimize weaning and extubation success in the critically ill. Intensive Care Medicine. 2020;46(12):2461-3.
10. Windisch W, Dellweg D, Geiseler J, Westhoff M, Pfeifer M, Suchi S, et al. Prolonged weaning from mechanical ventilation: results from specialized weaning centers—a registry-based study from the WeanNet Initiative. Deutsches Ärzteblatt International. 2020;117(12):197.
11. El-Baradey GF, El-Shmaa NS, Ganna SA. Can integrative weaning index be a routine predictor for weaning success? Indian Journal of Critical Care Medicine: Peer-reviewed, Official Publication of Indian Society of Critical Care Medicine. 2015;19(12):703.
12. Wang Y, Lei L, Yang H, He S, Hao J, Liu T, et al. Weaning critically ill patients from mechanical ventilation: a protocol from a multicenter retrospective cohort study. Journal of Thoracic Disease. 2022;14(1):199.
13. Zein H, Baratloo A, Negida A, Safari S. Ventilator weaning and spontaneous breathing trials; an educational review. Emergency. 2016;4(2):65.
14. Souza LCd, Lugon JR. The rapid shallow breathing index as a predictor of successful mechanical ventilation weaning: clinical utility when calculated from ventilator data. Jornal Brasileiro de Pneumologia. 2015;41:530-5.
15. Tu C-S, Chang C-H, Chang S-C, Lee C-S, Chang C-T. A decision for predicting successful extubation of patients in intensive care unit. BioMed research international. 2018;2018.
16. Alam MJ, Roy S, Iktidar MA, Padma FK, Nipun KI, Chowdhury S, et al. Diaphragm ultrasound as a better predictor of successful extubation from mechanical ventilation than rapid shallow breathing index. Acute and Critical Care. 2022;37(1):94-100.
17. Heunks LM, Doorduin J, van der Hoeven JG. Monitoring and preventing diaphragm injury. Curr Opin Crit Care. 2015;21(1):34-41.
18. Oppersma E, Hatam N, Doorduin J, van der Hoeven JG, Marx G, Goetzenich A, et al. Functional assessment of the diaphragm by speckle tracking ultrasound during inspiratory loading. J Appl Physiol (1985). 2017;123(5):1063-70.
19. Umbrello M, Formenti P, Lusardi AC, Guanziroli M, Caccioppola A, Coppola S, et al. Oesophageal pressure and respiratory muscle ultrasonographic measurements indicate inspiratory effort during pressure support ventilation. Br J Anaesth. 2020;125(1):e148-e57.
20. Orde SR, Boon AJ, Firth DG, Villarraga HR, Sekiguchi H. Diaphragm assessment by two dimensional speckle tracking imaging in normal subjects. BMC anesthesiology. 2015;16(1):1-8.
21. Supinski GS, Callahan LA. Diaphragm weakness in mechanically ventilated critically ill patients. Crit Care. 2013;17(3):R120.
22. Doorduin J, Roesthuis LH, Jansen D, Van Der Hoeven JG, Van Hees HWH, Heunks LMA. Respiratory muscle effort during expiration in successful and failed weaning from mechanical ventilation. Anesthesiology. 2018;129(3):490-501.
23. de Vries H, Jonkman A, Shi Z-H, Spoelstra-de Man A, Heunks L. Assessing breathing effort in mechanical ventilation: physiology and clinical implications. Annals of Translational Medicine. 2018;6(19).
24. Umbrello M, Formenti P, Longhi D, Galimberti A, Piva I, Pezzi A, et al. Diaphragm ultrasound as indicator of respiratory effort in critically ill patients undergoing assisted mechanical ventilation: a pilot clinical study. Crit Care. 2015;19(1):161.
25. Supinski GS, Netzel PF, Westgate PM, Schroder EA, Wang L, Callahan LA. Magnetic twitch assessment of diaphragm and quadriceps weakness in critically ill mechanically ventilated patients. Respir Physiol Neurobiol. 2022;295:103789.
26. Hermans G, Agten A, Testelmans D, Decramer M, Gayan-Ramirez G. Increased duration of mechanical ventilation is associated with decreased diaphragmatic force: a prospective observational study. Crit Care. 2010;14(4):R127.
27. Buscher H, Valta P, Boie T, Hinz J, Moerer O, Sydow M, et al. Assessment of diaphragmatic function with cervical magnetic stimulation in critically ill patients. Anaesth Intensive Care. 2005;33(4):483-91.
28. Demoule A, Molinari N, Jung B, Prodanovic H, Chanques G, Matecki S, et al. Patterns of diaphragm function in critically ill patients receiving prolonged mechanical ventilation: a prospective longitudinal study. Ann Intensive Care. 2016;6(1):75.
29. Watson AC, Hughes PD, Louise Harris M, Hart N, Ware RJ, Wendon J, et al. Measurement of twitch transdiaphragmatic, esophageal, and endotracheal tube pressure with bilateral anterolateral magnetic phrenic nerve stimulation in patients in the intensive care unit. Crit Care Med. 2001;29(7):1325-31.
30. Lassola S, Miori S, Sanna A, Cucino A, Magnoni S, Umbrello M. Central venous pressure swing outperforms diaphragm ultrasound as a measure of inspiratory effort during pressure support ventilation in COVID-19 patients. J Clin Monit Comput. 2022;36(2):461-71.
31. Saccheri C, Morawiec E, Delemazure J, Mayaux J, Dubé BP, Similowski T, et al. ICU-acquired weakness, diaphragm dysfunction and long-term outcomes of critically ill patients. Ann Intensive Care. 2020;10(1):1.
32. Lecronier M, Jung B, Molinari N, Pinot J, Similowski T, Jaber S, et al. Severe but reversible impaired diaphragm function in septic mechanically ventilated patients. Ann Intensive Care. 2022;12(1):34.
33. Demoule A, Jung B, Prodanovic H, Molinari N, Chanques G, Coirault C, et al. Diaphragm Dysfunction on Admission to the Intensive Care Unit Prevalence, Risk Factors, and Prognostic Impact-A

Prospective Study. American Journal of Respiratory and Critical Care Medicine. 2013;188(2):213-9.
34. Barwing J, Pedroni C, Olgemöller U, Quintel M, Moerer O. Electrical activity of the diaphragm (EAdi) as a monitoring parameter in difficult weaning from respirator: a pilot study. Crit Care. 2013;17(4):R182.
35. Sklar MC, Madotto F, Jonkman A, Rauseo M, Soliman I, Damiani LF, et al. Duration of diaphragmatic inactivity after endotracheal intubation of critically ill patients. Crit Care. 2021;25(1):26.
36. Pozzi M, Rezoagli E, Bronco A, Rabboni F, Grasselli G, Foti G, et al. Accessory and Expiratory Muscles Activation During Spontaneous Breathing Trial: A Physiological Study by Surface Electromyography. Front Med (Lausanne). 2022;9:814219.
37. Ghasem Hanafi M, Kiani H, Rashidi M. Evaluation of Diaphragm dysfunction to Predict Extubation Time of Critically Ill Patients in ICU with Ultrasonography. Pakistan Journal of Medical and Health Sciences. 2020;14(2):924-8.
38. DiNino E, Gartman EJ, Sethi JM, McCool FD. Diaphragm ultrasound as a predictor of successful extubation from mechanical ventilation. Thorax. 2014;69(5):423-7.
39. Kilapong B, Aditianingsih D, Sedono R, Sugiarto A, Salamah T. Diaphragm muscle thinning in mechanically ventilated critically ill patients. J Pak Med Assoc. 2021;71(Suppl 2)(2):S78-s83.
40. Goligher EC, Fan E, Herridge MS, Murray A, Vorona S, Brace D, et al. Evolution of Diaphragm Thickness during Mechanical Ventilation. Impact of Inspiratory Effort. Am J Respir Crit Care Med. 2015;192(9):1080-8.
41. Francis CA, Hoffer JA, Reynolds S. Ultrasonographic Evaluation of Diaphragm Thickness During Mechanical Ventilation in Intensive Care Patients. Am J Crit Care. 2016;25(1):e1-8.
42. Zambon M, Beccaria P, Matsuno J, Gemma M, Frati E, Colombo S, et al. Mechanical Ventilation and Diaphragmatic Atrophy in Critically Ill Patients: An Ultrasound Study. Crit Care Med. 2016;44(7):1347-52.
43. Schepens T, Verbrugghe W, Dams K, Corthouts B, Parizel PM, Jorens PG. The course of diaphragm atrophy in ventilated patients assessed with ultrasound: a longitudinal cohort study. Crit Care. 2015;19:422.
44. Vivier E, Roussey A, Doroszewski F, Rosselli S, Pommier C, Carteaux G, et al. Atrophy of Diaphragm and Pectoral Muscles in Critically Ill Patients. Anesthesiology. 2019;131(3):569-79.
45. Er B, Simsek M, Yildirim M, Halacli B, Ocal S, Ersoy EO, et al. Association of baseline diaphragm, rectus femoris and vastus intermedius muscle thickness with weaning from mechanical ventilation. Respir Med. 2021;185:106503.
46. Sklar MC, Dres M, Fan E, Rubenfeld GD, Scales DC, Herridge MS, et al. Association of Low Baseline Diaphragm Muscle Mass With Prolonged Mechanical Ventilation and Mortality Among Critically Ill Adults. JAMA Netw Open. 2020;3(2):e1921520.
47. Ali ER, Mohamad AM. Diaphragm ultrasound as a new functional and morphological index of outcome, prognosis and discontinuation from mechanical ventilation in critically ill patients and evaluating the possible protective indices against VIDD. Egyptian Journal of Chest Diseases and Tuberculosis. 2017;66(2):339-51.
48. Lu Z, Ge H, Xu L, Guo F, Zhang G, Wu Y. Alterations in diaphragmatic function assessed by ultrasonography in mechanically ventilated patients with sepsis. J Clin Ultrasound. 2019;47(4):206-11.
49. Baldwin CE, Bersten AD. Alterations in respiratory and limb muscle strength and size in patients with sepsis who are mechanically ventilated. Phys Ther. 2014;94(1):68-82.
50. Bertoni M, Telias I, Urner M, Long M, Del Sorbo L, Fan E, et al. A novel non-invasive method to detect excessively high respiratory effort and dynamic transpulmonary driving pressure during mechanical ventilation. Crit Care. 2019;23(1):346.
51. Gok F, Mercan A, Kilicaslan A, Sarkilar G, Yosunkaya A. Diaphragm and Lung Ultrasonography During Weaning From Mechanical Ventilation in Critically Ill Patients. Cureus. 2021;13(5):e15057.
52. Varón-Vega F, Hernández Á, López M, Cáceres E, Giraldo-Cadavid LF, Uribe-Hernandez AM, et al. Usefulness of diaphragmatic ultrasound in predicting extubation success. Med Intensiva (Engl Ed). 2021;45(4):226-33.
53. Goligher EC, Laghi F, Detsky ME, Farias P, Murray A, Brace D, et al. Measuring diaphragm thickness with ultrasound in mechanically ventilated patients: feasibility, reproducibility and validity. Intensive Care Med. 2015;41(4):642-9.
54. Goligher EC, Dres M, Fan E, Rubenfeld GD, Scales DC, Herridge MS, et al. Mechanical Ventilation-induced Diaphragm Atrophy Strongly Impacts Clinical Outcomes. Am J Respir Crit Care Med. 2018;197(2):204-13.
55. Mariani LF, Bedel J, Gros A, Lerolle N, Milojevic K, Laurent V, et al. Ultrasonography for Screening and Follow-Up of Diaphragmatic Dysfunction in the ICU: A Pilot Study. J Intensive Care Med. 2016;31(5):338-43.
56. Khan MT, Munawar K, Hussain SW, Qadeer A, Saeed ML, Shad ZS, et al. Comparing Ultrasound-based Diaphragmatic Excursion with Rapid Shallow Breathing Index as a Weaning Predictor. Cureus. 2018;10(12):e3710.
57. Flevari A, Lignos M, Konstantonis D, Armaganidis A. Diaphragmatic ultrasonography as an adjunct predictor tool of weaning success in patients with difficult and prolonged weaning. Minerva Anestesiol. 2016;82(11):1149-57.
58. Haji K, Haji D, Canty DJ, Royse AG, Green C, Royse CF. The impact of heart, lung and diaphragmatic ultrasound on prediction of failed extubation from mechanical ventilation in critically ill patients: a prospective observational pilot study. Crit Ultrasound J. 2018;10(1):13.
59. Xu X, Wu R, Zhang YJ, Li HW, He XH, Wang SM. Value of Combination of Heart, Lung, and Diaphragm Ultrasound in Predicting Weaning Outcome of Mechanical Ventilation. Med Sci Monit. 2020;26:e924885.
60. Garrido-Aguirre E, Ñamendys-Silva SA, Del Moral OR, Cortés-Soto CA, Romero-González JP. Diaphragmatic Ultrasonography, a Novel Approach in Critical Care: A Proposal for a New Weaning Index. Ultrasound Q. 2020;36(1):54-8.
61. Nugroho R, Mulyono I, George YWH. The accuracy of diaphragm thickening fraction, C-reactive protein, cumulative fluid balance, and rapid shallow breathing index in predicting the ease of weaning from

mechanical ventilation in critical patients in the ICU. Critical Care and Shock. 2022;25(1):1-6.
62. Darmawan A, Mulyono I, Wijaya AA. Role of cumulative fluid balance, intraabdominal pressure, diaphragm excursion, and neutrophil-lymphocyte ratio on the difficulty of the weaning process from mechanical ventilation in critically ill patients. Critical Care and Shock. 2022;25(2):61-6.
63. Tuinman PR, Jonkman AH, Dres M, Shi Z-H, Goligher EC, Goffi A, et al. Respiratory muscle ultrasonography: methodology, basic and advanced principles and clinical applications in ICU and ED patients—a narrative review. Intensive care medicine. 2020;46(4):594-605.
64. Hatam N, Goetzenich A, Rossaint R, Karfis I, Bickenbach J, Autschbach R, et al. A novel application for assessing diaphragmatic function by ultrasonic deformation analysis in noninvasively ventilated healthy young adults. Ultraschall in der Medizin-European Journal of Ultrasound. 2014;35(06):540-6.

Appendix A: Search terms

PubMed (MEDLINE):

(("Diaphragm"[Mesh] OR "Diaphragm"[tw] OR "Diaphragms"[tw] OR "Diaphragm*"[tw]) AND ("Critical Illness"[Mesh] OR "critically ill patients"[tw] OR "critically ill patient"[tw] OR "critically ill"[tw] OR "critical ill patients"[tw] OR "critical ill patients"[tw] OR "critical ill"[tw] OR "critical illness"[tw] OR "Ventilator-Induced Lung Injury"[Mesh] OR "Lung Injury"[Mesh:noexp] OR "Acute Lung Injury"[mesh] OR "lung injury"[tw] OR "lung injuries"[tw] OR "injured lung"[tw] OR "injured lungs"[tw] OR "Lung/injuries"[Mesh] OR "Respiratory Muscles/injuries"[Mesh]) AND ("prolonged mechanical ventilation"[tw] OR "Respiration, Artificial"[Mesh] OR "Ventilators, Mechanical"[Mesh] OR "mechanical ventilation"[tw] OR "Artificial Respirat*"[tw] OR "Artificial Respiration"[tw] OR "Mechanical Ventilat*"[tw] OR "Mechanical Ventilator"[tw] OR "Mechanical Ventilators"[tw] OR "Pulmonary Ventilator"[tw] OR "Pulmonary Ventilators"[tw] OR "Respirator"[tw] OR "Respirators"[tw] OR "Ventilator"[tw] OR "Ventilators"[tw] OR "Continuous Positive Airway Pressure"[tw] OR "High-Frequency Jet Ventilation"[tw] OR "High-Frequency Ventilation"[tw] OR "Interactive Ventilatory Support"[tw] OR "Intermittent Positive-Pressure Breathing"[tw] OR "Intermittent Positive-Pressure Ventilation"[tw] OR "Liquid Ventilation"[tw] OR "Noninvasive Ventilation"[tw] OR "One-Lung Ventilation"[tw] OR "Positive-Pressure Respiration"[tw] OR "Ventilator Weaning"[tw]) AND ("Monitoring, Physiologic"[Mesh] OR "Ultrasonography"[Mesh] OR "Magnetic Resonance Imaging"[Mesh] OR "Tomography, X-Ray Computed"[Mesh] OR "Electromyography"[Mesh] OR "monitoring"[tw] OR "monitor"[tw] OR "monitor*"[tw] OR "ultrasonography"[tw] OR "ultrasonogr*"[tw] OR "magnetic resonance imaging"[tw] OR "MRI"[tw] OR "MR imaging"[tw] OR "computed tomography"[tw] OR "neurally adjusted ventilatory assist"[tw] OR "NAVA"[tw] OR "electromyography"[tw] OR "electromyogr*"[tw] OR "EMG"[tw] OR "parameters"[tw] OR "parameter"[tw] OR "paramet*"[tw] OR "quantify"[tw] OR "quantification"[tw] OR "quantitation"[tw] OR "quantif*"[tw] OR "diaphragm function"[tw] OR "diaphragm function*"[tw] OR "diaphragm dysfunction"[tw] OR "diaphragm dysfunction*"[tw] OR "diaphragm strength"[tw] OR "diaphragm strength*"[tw] OR "thickness"[tw] OR "thickening"[tw] OR "strain"[tw] OR "excursion"[tw] OR "motion"[tw] OR "Algorithms"[Mesh] OR "Algorithms"[tw] OR "Algorithm"[tw] OR "algorithm*"[tw]))

Embase:

((exp *"Diaphragm"/ OR exp *"Diaphragm Movement"/ OR "Diaphragm".ti,ab OR "Diaphragms".ti,ab OR "Diaphragm*".ti,ab) AND (exp *"Critical Illness"/ OR exp *"critically ill patient"/ OR "critically ill patients".ti,ab OR "critically ill patient".ti,ab OR "critically ill".ti,ab OR "critical ill patients".ti,ab OR "critical ill patients".ti,ab OR "critical ill".ti,ab OR "critical illness".ti,ab OR exp *"Ventilator Induced Lung Injury"/ OR exp *"Lung Injury"/ OR exp *"Acute Lung Injury"/ OR "lung injury".ti,ab OR "lung injuries".ti,ab OR "injured lung".ti,ab OR "injured lungs".ti,ab) AND ("prolonged mechanical ventilation".ti,ab OR exp *"Artificial Ventilation"/ OR exp *"Mechanical Ventilators"/ OR "mechanical ventilation".ti,ab OR "Artificial Respirat*".ti,ab OR "Artificial Respiration".ti,ab OR "Mechanical Ventilat*".ti,ab OR "Mechanical Ventilator".ti,ab OR "Mechanical Ventilators".ti,ab OR "Pulmonary Ventilator".ti,ab OR "Pulmonary Ventilators".ti,ab OR "Respirator".ti,ab OR "Respirators".ti,ab OR exp *"Ventilator"/ OR "Ventilator".ti,ab OR "Ventilators".ti,ab OR "Continuous Positive Airway Pressure".ti,ab OR "High-Frequency Jet Ventilation".ti,ab OR "High-Frequency Ventilation".ti,ab OR "Interactive Ventilatory Support".ti,ab OR "Intermittent Positive-Pressure Breathing".ti,ab OR "Intermittent Positive-Pressure Ventilation".ti,ab OR "Liquid Ventilation".ti,ab OR "Noninvasive Ventilation".ti,ab OR "One-Lung Ventilation".ti,ab OR "Positive-Pressure Respiration".ti,ab OR "Ventilator Weaning".ti,ab) AND (exp *"Monitoring"/ OR exp *"Echography"/ OR exp *"Nuclear Magnetic Resonance Imaging"/ OR exp *"Computer Assisted Tomography"/ OR exp *"Electromyography"/ OR "monitoring".ti,ab OR "monitor".ti,ab OR "monitor*".ti,ab OR "ultrasonography".ti,ab OR "ultrasonogr*".ti,ab OR "magnetic resonance imaging".ti,ab OR "MRI".ti,ab OR "MR imaging".ti,ab OR "computed tomography".ti,ab OR "neurally adjusted ventilatory assist".ti,ab OR "NAVA".ti,ab OR "electromyography".ti,ab OR "electromyogr*".ti,ab OR "EMG".ti,ab OR exp *"parameters"/ OR "parameters".ti,ab OR "parameter".ti,ab OR "paramet*".ti,ab OR "quantify".ti,ab OR "quantification".ti,ab OR exp *"quantitative analysis"/ OR "quantitation".ti,ab OR "quantif*".ti,ab OR "diaphragm function".ti,ab OR "diaphragm function*".ti,ab OR "diaphragm dysfunction".ti,ab OR "diaphragm dysfunction*".ti,ab OR "diaphragm strength".ti,ab OR "diaphragm strength*".ti,ab OR "thickness".ti,ab OR "thickening".ti,ab OR "strain".ti,ab OR "excursion".ti,ab OR "motion".ti,ab OR exp *"Algorithm"/ OR "Algorithms".ti,ab OR "Algorithm".ti,ab OR "algorithm*".ti,ab)) NOT (conference review or conference abstract).pt

Web of Science:

((TI=("Diaphragm" OR "Diaphragm Movement" OR "Diaphragm" OR "Diaphragms" OR "Diaphragm*") OR AK=("Diaphragm" OR "Diaphragm Movement" OR "Diaphragm" OR "Diaphragms" OR "Diaphragm*") OR AB=("Diaphragm" OR "Diaphragm Movement" OR "Diaphragm" OR "Diaphragms" OR "Diaphragm*")) AND (TI=("Critical Illness" OR "critically ill patient" OR "critically ill patients" OR "critically ill patient" OR "critically ill" OR "critical ill patients" OR "critical ill patients" OR "critical ill" OR "critical illness" OR "Ventilator Induced Lung Injury" OR "Lung Injury" OR "Acute Lung Injury" OR "lung injury" OR "lung injuries" OR "injured lung" OR "injured lungs") OR AK=("Critical Illness" OR "critically ill patient" OR "critically ill patients" OR "critically ill patient" OR "critically ill" OR "critical ill patients" OR "critical ill patients" OR "critical ill" OR "critical illness" OR "Ventilator Induced Lung Injury" OR "Lung Injury" OR "Acute Lung Injury" OR "lung injury" OR "lung injuries" OR "injured lung" OR "injured lungs") OR AB=("Critical Illness" OR "critically ill patient" OR "critically ill patients" OR "critically ill patient" OR "critically ill" OR "critical ill patients" OR "critical ill patients" OR "critical ill" OR "critical illness" OR "Ventilator Induced Lung Injury" OR "Lung Injury" OR "Acute Lung Injury" OR "lung injury" OR "lung injuries" OR "injured lung" OR "injured lungs")) AND (TI=("prolonged mechanical ventilation" OR "Artificial Ventilation" OR "Mechanical Ventilators" OR "mechanical ventilation" OR "Artificial Respirat*" OR "Artificial Respiration" OR "Mechanical Ventilat*" OR "Mechanical Ventilator" OR "Mechanical Ventilators" OR "Pulmonary Ventilator" OR "Pulmonary Ventilators" OR "Respirator" OR "Respirators" OR "Ventilator" OR "Ventilator" OR "Ventilators" OR "Continuous Positive Airway Pressure" OR "High-Frequency Jet Ventilation" OR "High-Frequency Ventilation" OR "Interactive Ventilatory Support" OR "Intermittent Positive-Pressure Breathing" OR "Intermittent Positive-Pressure Ventilation" OR "Liquid Ventilation" OR "Noninvasive Ventilation" OR "One-Lung Ventilation" OR "Positive-Pressure Respiration" OR "Ventilator Weaning") OR AK=("prolonged mechanical ventilation" OR "Artificial Ventilation" OR "Mechanical Ventilators" OR "mechanical ventilation" OR "Artificial Respirat*" OR "Artificial Respiration" OR "Mechanical Ventilat*" OR "Mechanical Ventilator" OR "Mechanical Ventilators" OR "Pulmonary Ventilator" OR "Pulmonary Ventilators" OR "Respirator" OR "Respirators" OR "Ventilator" OR "Ventilator" OR "Ventilators" OR "Continuous Positive Airway Pressure" OR "High-Frequency Jet Ventilation" OR "High-Frequency Ventilation" OR "Interactive Ventilatory Support" OR "Intermittent Positive-Pressure Breathing" OR "Intermittent Positive-Pressure Ventilation" OR "Liquid Ventilation" OR "Noninvasive Ventilation" OR "One-Lung Ventilation" OR "Positive-Pressure Respiration" OR "Ventilator Weaning") OR AB=("prolonged mechanical ventilation" OR "Artificial Ventilation" OR "Mechanical Ventilators" OR "mechanical ventilation" OR "Artificial Respirat*" OR "Artificial Respiration" OR "Mechanical Ventilat*" OR "Mechanical Ventilator" OR "Mechanical Ventilators" OR "Pulmonary Ventilator" OR "Pulmonary Ventilators" OR "Respirator" OR "Respirators" OR "Ventilator" OR "Ventilator" OR "Ventilators" OR "Continuous Positive Airway Pressure" OR "High-Frequency Jet Ventilation" OR "High-Frequency Ventilation" OR "Interactive Ventilatory Support" OR "Intermittent Positive-Pressure Breathing" OR "Intermittent Positive-Pressure Ventilation" OR "Liquid Ventilation" OR "Noninvasive Ventilation" OR "One-Lung Ventilation" OR "Positive-Pressure Respiration" OR "Ventilator Weaning")) AND (TI=("Monitoring" OR "Echography" OR "Nuclear Magnetic Resonance Imaging" OR "Computer Assisted Tomography" OR "Electromyography" OR "monitoring" OR "monitor" OR "monitor*" OR "ultrasonography" OR "ultrasonogr*" OR "magnetic resonance imaging" OR "MRI" OR "MR imaging" OR "computed tomography" OR "neurally adjusted ventilatory assist" OR "NAVA" OR "electromyography" OR "electromyogr*" OR "EMG" OR "parameters" OR "parameters" OR "parameter" OR "paramet*" OR "quantify" OR "quantification" OR "quantitative analysis" OR "quantitation" OR "quantif*" OR "diaphragm function" OR "diaphragm function*" OR "diaphragm dysfunction" OR "diaphragm dysfunction*" OR "diaphragm strength" OR "diaphragm strength*" OR "thickness" OR "thickening" OR "strain" OR "excursion" OR "motion" OR "Algorithm" OR "Algorithms" OR "Algorithm" OR "algorithm*") OR AK=("Monitoring" OR "Echography" OR "Nuclear Magnetic Resonance Imaging" OR "Computer Assisted Tomography" OR "Electromyography" OR "monitoring" OR "monitor" OR "monitor*" OR "ultrasonography" OR "ultrasonogr*" OR "magnetic resonance imaging" OR "MRI" OR "MR imaging" OR "computed tomography" OR "neurally adjusted ventilatory assist" OR "NAVA" OR "electromyography" OR "electromyogr*" OR "EMG" OR "parameters" OR "parameters" OR "parameter" OR "paramet*" OR "quantify" OR "quantification" OR "quantitative analysis" OR "quantitation" OR "quantif*" OR "diaphragm function" OR "diaphragm function*" OR "diaphragm dysfunction" OR "diaphragm dysfunction*" OR "diaphragm strength" OR "diaphragm strength*" OR "thickness" OR "thickening" OR "strain" OR "excursion" OR "motion" OR "Algorithm" OR "Algorithms" OR "Algorithm" OR "algorithm*") OR AB=("Monitoring" OR "Echography" OR "Nuclear Magnetic Resonance Imaging" OR "Computer Assisted Tomography" OR "Electromyography" OR "monitoring" OR "monitor" OR "monitor*" OR "ultrasonography" OR "ultrasonogr*" OR "magnetic resonance imaging" OR "MRI" OR "MR imaging" OR "computed tomography" OR "neurally adjusted ventilatory assist" OR "NAVA" OR "electromyography" OR "electromyogr*" OR "EMG" OR "parameters" OR "parameters" OR "parameter" OR "paramet*" OR "quantify" OR "quantification" OR "quantitative analysis" OR "quantitation" OR "quantif*" OR "diaphragm function" OR "diaphragm function*" OR "diaphragm dysfunction" OR "diaphragm dysfunction*" OR "diaphragm strength" OR "diaphragm strength*" OR "thickness" OR "thickening" OR "strain" OR "excursion" OR "motion" OR "Algorithm" OR "Algorithms" OR "Algorithm" OR "algorithm*"))) NOT DT=(meeting abstract)

Emcare:

((exp *"Diaphragm"/ OR exp *"Diaphragm Movement"/ OR "Diaphragm".ti,ab OR "Diaphragms".ti,ab OR "Diaphragm*".ti,ab) AND (exp *"Critical Illness"/ OR exp *"critically ill patient"/ OR "critically ill patients".ti,ab OR "critically ill patient".ti,ab OR "critically ill".ti,ab OR "critical ill patients".ti,ab OR "critical ill patients".ti,ab OR "critical ill".ti,ab OR "critical illness".ti,ab OR exp *"Ventilator Induced Lung Injury"/ OR exp *"Lung Injury"/ OR exp *"Acute Lung Injury"/ OR "lung injury".ti,ab OR "lung injuries".ti,ab OR "injured lung".ti,ab OR "injured lungs".ti,ab) AND ("prolonged mechanical ventilation".ti,ab OR exp *"Artificial Ventilation"/ OR exp *"Mechanical Ventilators"/ OR "mechanical ventilation".ti,ab OR "Artificial Respirat*".ti,ab OR "Artificial Respiration".ti,ab OR "Mechanical Ventilat*".ti,ab OR "Mechanical Ventilator".ti,ab OR "Mechanical Ventilators".ti,ab OR "Pulmonary Ventilator".ti,ab OR "Pulmonary Ventilators".ti,ab OR "Respirator".ti,ab OR "Respirators".ti,ab OR exp *"Ventilator"/ OR "Ventilator".ti,ab OR "Ventilators".ti,ab OR "Continuous Positive Airway Pressure".ti,ab OR "High-Frequency Jet Ventilation".ti,ab OR "High-Frequency Ventilation".ti,ab OR "Interactive Ventilatory Support".ti,ab OR "Intermittent Positive-Pressure Breathing".ti,ab OR "Intermittent Positive-Pressure Ventilation".ti,ab OR "Liquid Ventilation".ti,ab OR "Noninvasive Ventilation".ti,ab OR "One-Lung Ventilation".ti,ab OR "Positive-Pressure Respiration".ti,ab OR "Ventilator Weaning".ti,ab) AND (exp *"Monitoring"/ OR exp *"Echography"/ OR exp *"Nuclear Magnetic Resonance Imaging"/ OR exp *"Computer Assisted Tomography"/ OR exp *"Electromyography"/ OR "monitoring".ti,ab OR "monitor".ti,ab OR "monitor*".ti,ab OR "ultrasonography".ti,ab OR "ultrasonogr*".ti,ab OR "magnetic resonance imaging".ti,ab OR "MRI".ti,ab OR "MR imaging".ti,ab OR "computed tomography".ti,ab OR "neurally adjusted ventilatory assist".ti,ab OR "NAVA".ti,ab OR "electromyography".ti,ab OR "electromyogr*".ti,ab OR "EMG".ti,ab OR exp *"parameters"/ OR "parameters".ti,ab OR "parameter".ti,ab OR "paramet*".ti,ab OR "quantify".ti,ab OR "quantification".ti,ab OR exp *"quantitative analysis"/ OR "quantitation".ti,ab OR "quantif*".ti,ab OR "diaphragm function".ti,ab OR "diaphragm function*".ti,ab OR "diaphragm dysfunction".ti,ab OR "diaphragm dysfunction*".ti,ab OR "diaphragm strength".ti,ab OR "diaphragm strength*".ti,ab OR "thickness".ti,ab OR "thickening".ti,ab OR "strain".ti,ab OR "excursion".ti,ab OR "motion".ti,ab OR exp *"Algorithm"/ OR "Algorithms".ti,ab OR "Algorithm".ti,ab OR "algorithm*".ti,ab))

Cochrane Library:

(("Diaphragm" OR "Diaphragm Movement" OR "Diaphragm" OR "Diaphragms" OR "Diaphragm*") AND ("Critical Illness" OR "critically ill patient" OR "critically ill patients" OR "critically ill patient" OR "critically ill" OR "critical ill patients" OR "critical ill patients" OR "critical ill" OR "critical illness" OR "Ventilator Induced Lung Injury" OR "Lung Injury" OR "Acute Lung Injury" OR "lung injury" OR "lung injuries" OR "injured lung" OR "injured lungs") AND ("prolonged mechanical ventilation" OR "Artificial Ventilation" OR "Mechanical Ventilators" OR "mechanical ventilation" OR "Artificial Respirat*" OR "Artificial Respiration" OR "Mechanical Ventilat*" OR "Mechanical Ventilator" OR "Mechanical Ventilators" OR "Pulmonary Ventilator" OR "Pulmonary Ventilators" OR "Respirator" OR "Respirators" OR "Ventilator" OR "Ventilator" OR "Ventilators" OR "Continuous Positive Airway Pressure" OR "High Frequency Jet Ventilation" OR "High Frequency Ventilation" OR "Interactive Ventilatory Support" OR "Intermittent Positive Pressure Breathing" OR "Intermittent Positive Pressure Ventilation" OR "Liquid Ventilation" OR "Noninvasive Ventilation" OR "One Lung Ventilation" OR "Positive Pressure Respiration" OR "Ventilator Weaning") AND ("Monitoring" OR "Echography" OR "Nuclear Magnetic Resonance Imaging" OR "Computer Assisted Tomography" OR "Electromyography" OR "monitoring" OR "monitor" OR "monitor*" OR "ultrasonography" OR "ultrasonogr*" OR "magnetic resonance imaging" OR "MRI" OR "MR imaging" OR "computed tomography" OR "neurally adjusted ventilatory assist" OR "NAVA" OR "electromyography" OR "electromyogr*" OR "EMG" OR "parameters" OR "parameters" OR "parameter" OR "paramet*" OR "quantify" OR "quantification" OR "quantitative analysis" OR "quantitation" OR "quantif*" OR "diaphragm function" OR "diaphragm function*" OR "diaphragm dysfunction" OR "diaphragm dysfunction*" OR "diaphragm strength" OR "diaphragm strength*" OR "thickness" OR "thickening" OR "strain" OR "excursion" OR "motion" OR "Algorithm" OR "Algorithms" OR "Algorithm" OR "algorithm*")):ti,ab,kw

B

Ultrasound protocol UTOPIA study


Utopia

Background and introduction

Mechanical ventilation is, albeit lifesaving, damaging to the lung and may result in ventilator induced lung injury (VILI). Patients who are mechanically ventilated and have underlying lung abnormalities, such as consolidations, atelectasis or ARDS may benefit from lung recruitment maneuvers and higher PEEP levels to open up the lung and keep it open. A lung recruitment maneuver will result in more open lung but may also result in overextension of healthy parts of lung which may damage these parts.

The prevention of VILI is currently an important topic in critical care. Esophageal pressure measurements has been studied as a tool to prevent VILI that represents the changes in pleural pressure. However, this technique cannot give a good approximation of regional overdistension due to the uneven distribution of air delivery in patients with acute lung injury. Regional overdistention is associated with higher mortality due to lung damage and possible activation of cytokine storm resulting in multi organ failure.

The holy grail of mechanical ventilation is therefore to find the ventilator setting which maximally opens the lung parts which are closed without overextending the lung parts which are open. Currently this may only be reliably done with serial CT scanning or impedance measurements. However, we believe that using ultrasound we may also be able to measure lung features regionally. Lung features are distinctive patterns in an image that could say something about the condition of the lung. One example is the B line quantification algorithms that quantify lung fluid by counting comet trails artefacts from the pleura. Using ultrasound, we may be able to ascertain whether lung parts that were closed become opened up by scoring the level of atelectasis, consolidations and open lung all over the lungs and we may be able to measure overextension of the already open lung parts by quantifying lung sliding using speckle tracking techniques. Lung sliding is dynamic hyperechoic line in the image that occurred due to the visceral pleura moves against the parietal pleura with respiration.

The study aims therefore to investigate the effects of PEEP on lung sliding with the goal to use ultrasound to optimize mechanical ventilation. Secondary aim is to extract additional features to monitor diagraph movement and strain for example. The research will take place at the Leiden University Medical Center (LUMC) at the Intensive Care department. The pilot study is a collaboration between the hospital LUMC and manufacturer Philips. Ultrasound (US) imaging is used to investigate lung physiology and mechanics and specifically lung sliding. US is a non-radiating imaging modality that uses ultrasonic sound waves to measure tissue density and is clinically proven safe for humans.

Method

COVID group:

Patient is confirmed correct sedated and laid in supine position. A Hamilton data recording device is attached to the ventilator and activated.

1. Place Hamilton dongle in the serial port of the Hamilton C6 ventilator. **Use only the dongle with the green cable!.**
2. Click on start
3. Switch to wave mode
4. Click on start
5. Lights goes off. After +- 15 sec a small flickering of light indicate correct functionality.

6. For the image acquisition, we use a lumify S4-1 transducer in combination with a Samsung galaxy tab that is registered as a medical device. **Use only the smaller tablet (These tablets can only export images from the USB C port)**. First step is to request a lung ultrasound from the commando centrum. Then select the **Lung preset** and Select the patient info in the tablet by clicking new patient and 'zoekresultaten'. Furthermore, Fill the research number (as shown in a table below in section Administration) in as addition to the patient information box 'description'. Choose B-line feature. Then, the acquisition will take place in the following order:

- R1 = Upper anterior right lung
- R2 = Lower anterior right lung
- R3 = Upper lateral right lung
- R4 = Lower lateral right lung
- R5 = Upper posterior right lung
- R6 = Lower posterior right lung
- RD = Diagraph image right lung
- L1 = Upper anterior left lung
- L2 = Lower anterior left lung
- L3 = Upper lateral left lung
- L4 = Lower lateral left lung
- L5 = Upper posterior left lung
- L6 = Lower posterior left lung
- LD = Diagraph image left lung

Please check every image with the location code! A graphical representation of the location codes are visible in figure 1.

The duration of each acquisition is 7 seconds (check the settings).

7. Export data to DICOM store.
8. Click stop on the Hamilton dongle and remove the dongle.
9. Clean patient and equipment.
10. Fill in all requested information in the table below in section administration.

The data from the lumify is extracted with a USB flash drive to a secured server at the end of the day. Than the USB drive is formatted correctly after use. Same applied for the ventilator data.

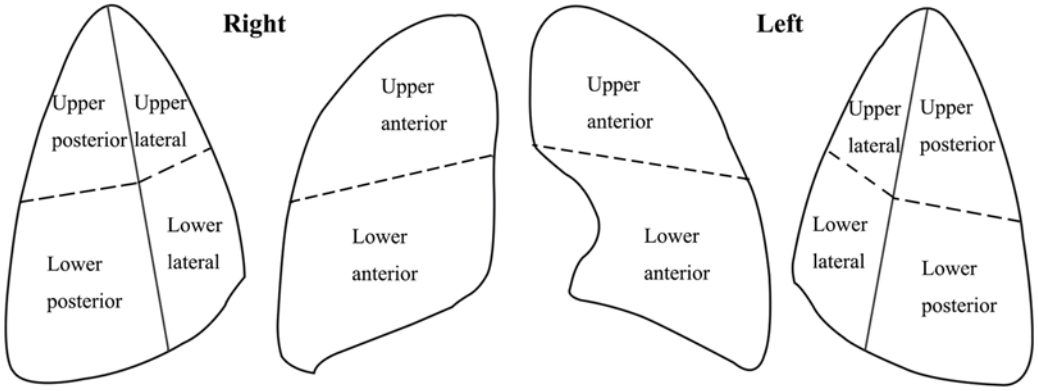

Figure 1: Each lung is separated into six quadrants: anterior, lateral and posterior zones that are further divided in an upper and lower zone. Image from Deng, Q., Cao, S., Wang, H. et al. Application of quantitative lung ultrasound instead of CT for monitoring COVID-19 pneumonia in pregnant women: a single-center retrospective study. BMC Pregnancy Childbirth 21, 259 (2021). https://doi.org/10.1186/s12884-021-03728-2

Administration

Research number	Date	Time (hh:mm)	Room number	Ventilator mode	Recruitment[1]	Diaphragm image (right,left,both,none)
R0005	18-11	13:30	8	SPONT	0	Right
R0006						
R0007						
R0008						

[1]Recruitment: 0 = without recruitment, 1= before recruitment, 2= during recruitment, 3 = 15 minutes after recruitment.

C

Algorithm experiments that did not succeed

Table C.1: Algorithm experiments that did not succeed

Algorithm	Problem to solve	Method tried	Why it did not succeed
DT	Cropping image of text and background	Automated method by intensity thresholding	Cropped too much in case of extensive acoustic shadowing
DT	Peritoneal line detection	Hough transform	Included many settings of constants that needed adaptation per individual clip
		Vesselness filter	Did not detect differences between pleural and peritoneal lines and other hyperechogenic lines in their neighborhood
DT	Segmentation of pleural and peritoneal border	Open-source region growing tool	Indicated threshold very specific in each individual diaphragm, hard to automate
IBST	Diaphragm mask definition	Using the two FBST tracking blocks as diaphragm masks	Too much affected by pleural and peritoneal line in view, causing incorrectly enhanced signal

Abbreviations: DT, diaphragm thickness; IBST, intensity-based speckle tracking; FBST, Fourier-based speckle tracking

D

Survey questions

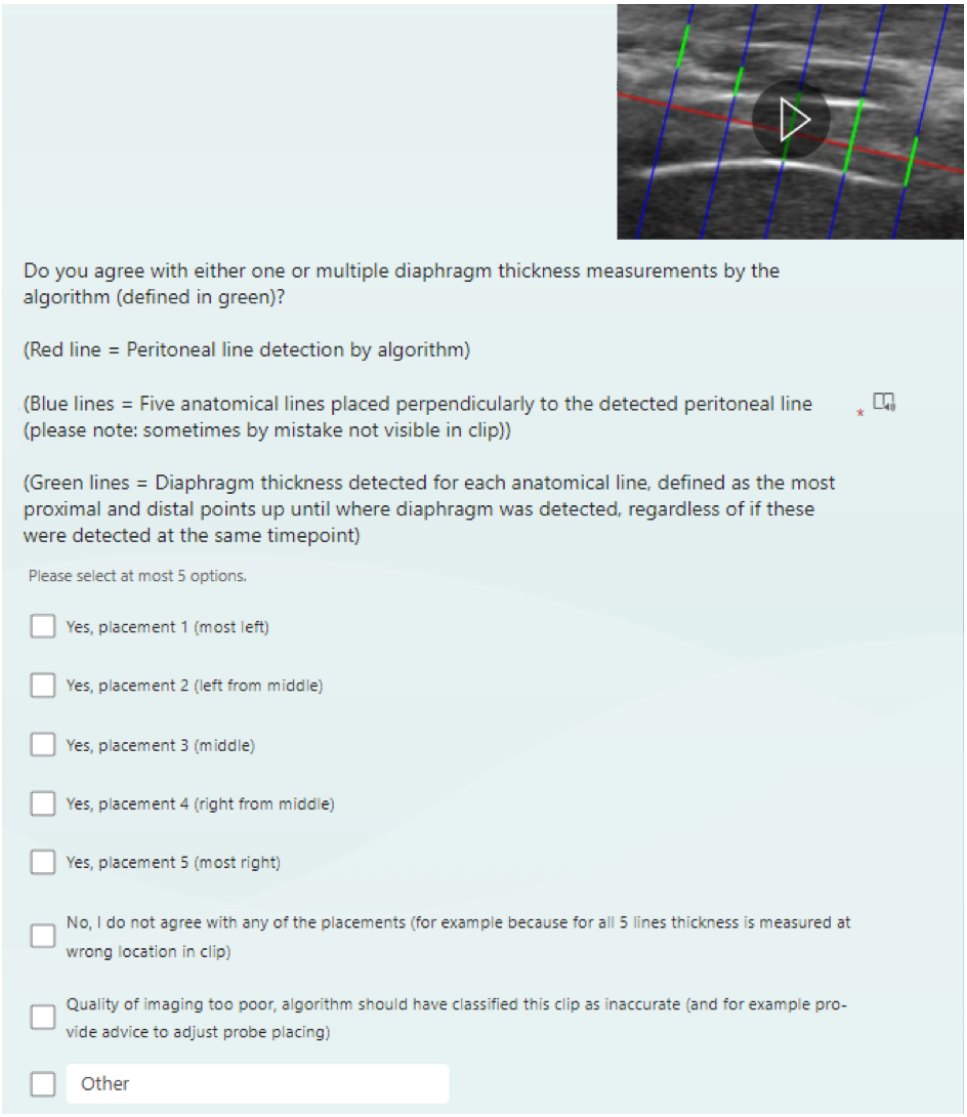

Figure D.1: Example survey question on an ultrasound video clip based on which the algorithm assessed diaphragm thickness

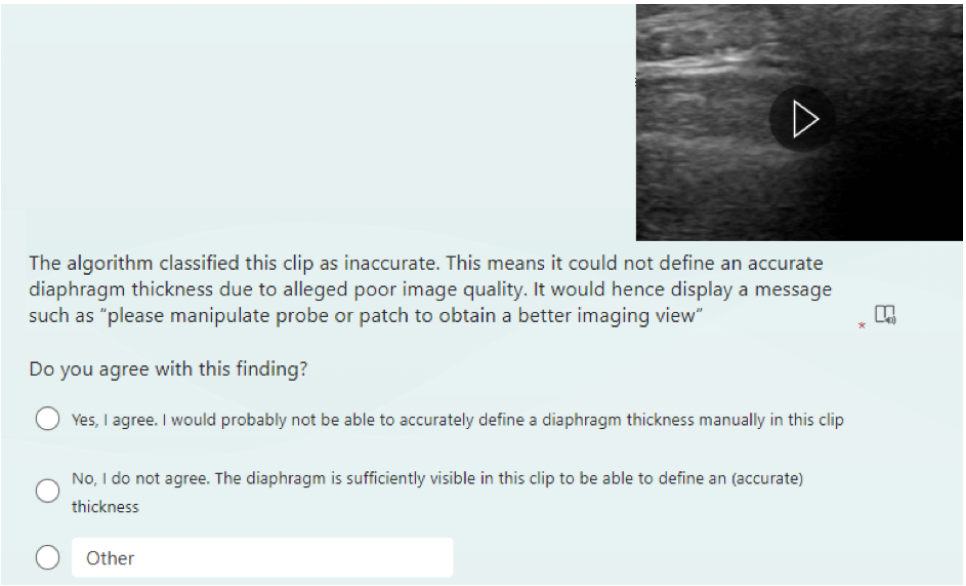

Figure D.2: Example survey question on an ultrasound video clip based on which the algorithm could not compute a diaphragm thickness

E

Common algorithm errors and challenges

E.1. DT quantification algorithm

E.1.1. Incorrect pleural line segmentation, often in case of hyperechogenic adipose or muscular tissue in proximity

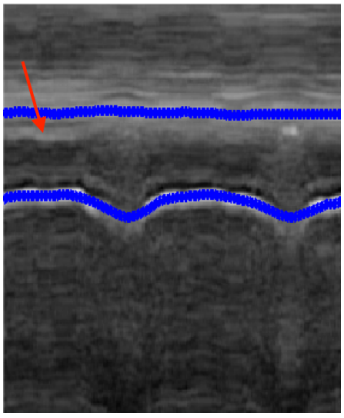

Figure E.1: Example of incorrect pleural line segmented in the first frames, with a red arrow pointing to the proper pleural line start

E.1.2. Too much tissue included in exaggerated pleural or peritoneal line

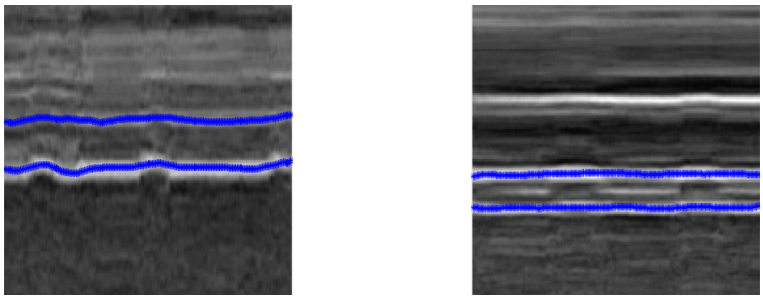

Figure E.2: Two examples of an exaggerated peritoneal line (left), and pleural and peritoneal line (right), where the algorithm may overestimate diaphragm thickness

E.2. IBST algorithm

E.2.1. Diaphragm mask too large, including pleural or peritoneal line, thereby overestimating movability signal

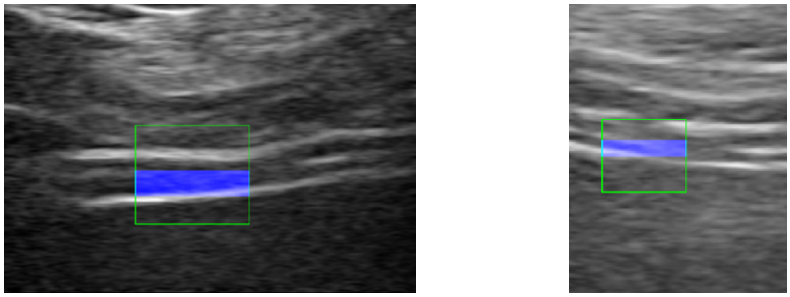

Figure E.3: Two examples of an overly large diaphragm mask including the peritoneal line

E.2.2. Segmentation of tendon instead of pleural or peritoneal line, resulting in a small diaphragm mask

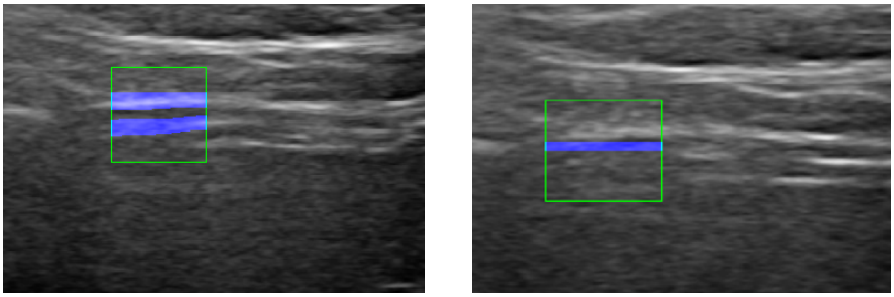

(a) Segmentation of central tendon instead of peritoneal line

(b) Resulting diaphragm mask of only half of desired area

Figure E.4: Example of tendon segmentation instead of peritoneal line resulting in a small diaphragm mask

E.2.3. Small diaphragm mask in thin diaphragms with exaggerated pleural and peritoneal lines

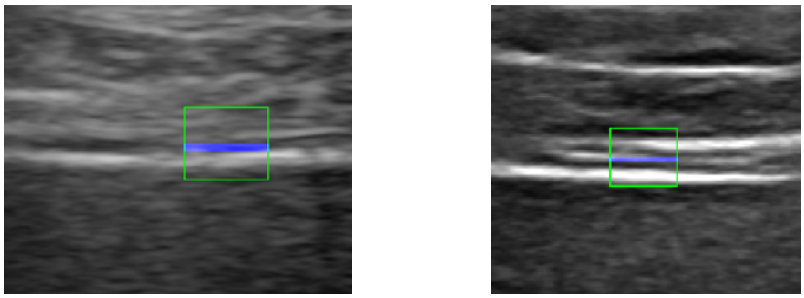

Figure E.5: Two examples of a small diaphragm mask in thin diaphragms with exaggerated pleural and peritoneal lines

F

DT, FBST and IBST algorithm variables, divided between genders and for two measurements over time

Table F.1: DT values of right hemidiaphragm by DT quantification algorithm, divided between genders

Variable	All subjects (*N* = 12)	Males (*N* = 8)	Females (*N* = 4)	*P*-value
DT_{min} (mm)	1.9 ± 0.4	1.9 ± 0.5	2.0 ± 0.3	0.788
DT_{max} (mm)	2.3 ± 0.5	2.3 ± 0.6	2.4 ± 0.4	0.914
DTF (%)	22.6 ± 10.9	23.5 ± 13.3	20.7 ± 3.8	0.594
AUC_{DT}	14.3 ± 3.0	14.1 ± 3.3	14.8 ± 2.5	0.748
GLS (%)	-32.0 ± 19.8	-33.8 ± 20.6	-28.5 ± 22.0	0.730
GLSR (%/s)	-6.6 ± 3.8	-7.1 ± 3.9	-5.5 ± 4.1	0.411
IBST score	26.2 ± 17.6	26.6 ± 15.1	25.0 ± 27.4	0.905

Abbreviations: DT_{min}, minimal diaphragm thickness; DT_{max}, maximal diaphragm thickness; DTF, diaphragm thickening factor; AUC_{DT}, area under the curve of diaphragm thickness signal over time; GLS, global longitudinal strain; GLSR, global longitudinal strain rate; IBST, intensity-based speckle tracking

Table F.2: DT values of right hemidiaphragm by DT quantification algorithm, for two measurements over time (on average 6 ± 1 days on MV between measurement 1 and 2)

Variable	Measurement 1	Measurement 2	*P*-value
DT_{min} (mm)	2.1 ± 0.4	1.7 ± 0.4	0.342
DT_{max} (mm)	2.6 ± 0.5	2.2 ± 0.5	0.362
DTF (%)	27.5 ± 29.6	25.0 ± 11.0	0.898
AUC_{DT}	15.7 ± 2.1	13.3 ± 2.9	0.320
GLS (%)	-27.9 ± 11.5	-49.5 ± 4.4	0.094
GLSR (%/s)	-7.7 ± 5.2	-8.1 ± 1.9	0.935
IBST score	24.7 ± 5.1	16.0 ± 9.4	0.327